

Silicon Chelation in Aqueous and Nonaqueous Media: The Furanoidic Diol Approach**

Xaver Kästele, Peter Klüfers,* Florian Kopp, Jörg Schuhmacher, and Martin Vogt^[a]

Abstract: Anhydroerythritol (AnEryt) shares some of its ligand properties with furanosides and furanoses. Its bonding to silicon centers of coordination number four, five, and six was studied by X-ray and NMR methods, and compared to silicon bonding of related compounds. Diphenyl(cycloalkylenedioxy)silanes show various degrees of oligomerization depending on the diol component involved. For example, Ph₂Si(*cis*-ChxdH₂) (**1**) and Ph₂Si-*{(R,R)-trans-ChxdH₂}* (**2**; Chxd = cyclohexanediol) are dimeric, Ph₂Si(AnErytH₂) (**3**) is monomeric, and Ph₂Si(L-AnThreH₂) (**4**; AnThre = anhydrothreitol) is trimeric both in the solid state and in solution. Ph₂Si(*cis*-CptdH₂) (**5**) (Cptd = cyclopentenediol)

is monomeric in solution but dimerizes on crystallization. Si(AnErytH₂)₂ (**6**) and Si(*cis*-CptdH₂)₂ (**7**) are monomeric spiro compounds in solution but are pentacoordinate dimers in the crystalline state. Pentacoordinate silicate ions are found in A[Si(OH)(AnErytH₂)₂] (A = Na, **8a**; Rb, **8b**; Cs, **8c**). Related compounds are formed by substitution of the hydroxo by a phenyl ligand. K[SiPh(AnErytH₂)₂] \cdot 1/2 MeOH (**9**) is a prototypical example as it shows the two most significant isomers in one crystal structure: the *syn/anti* and the

anti/anti form (*syn* and *anti* define the oxolane ring orientation close to, or apart from, the monodentate ligand, respectively). *syn/anti* Isomerism generally rules the appearance of the NMR spectra of pentacoordinate silicates of furanos(id)e ligands. NMR spectroscopic data are presented for various pentacoordinate bis(diolato)silicates of adenosine, cytidine, methyl- β -D-ribofuranoside, and ribose. In even more basic solutions, hexacoordinate silicates are enriched. Preliminary X-ray analyses are presented for Cs₂[Si(CydH₂)₃] \cdot 21.5 H₂O (**10**) and Cs₂[Si(*cis*-InsH₂)₃] \cdot *cis*-Ins \cdot 8 H₂O (**11**) (Cyd = cytidine, Ins = inositol).

Keywords: carbohydrates • NMR spectroscopy • Si ligands • silicates • spiro compounds

Introduction

Carbohydrates are polyfunctional molecules. Synthetic chemistry thus focuses on the regioselectivity of carbohydrate transformations. Although metal catalysis appears to be a promising way to achieve selectivity, the basic problem remains the same when designing a catalytic reaction: which functional group is the prevalent metal-binding site? This

problem is particularly obvious with the reducing sugars—the aldoses and ketoses (glycoses)—as they lack configurational stability. Thus, the question of (semi)metal bonding continues: which functional group of which glucose isomer provides a suitable binding site? Our knowledge of this subject is rather limited, particularly with respect to X-ray analyses. The metal-binding sites of aldoses with special O-atom patterns were the first to be determined. Along with Taylor and Water's pioneering work on the structure of a lyxose-molybdenum complex,^[1] the binucleating ability of mannose towards trivalent metal ions is a further example of strong metal binding that is, however, restricted exclusively to one special sugar.^[2,3] More general rules for assessing the (semi)-metal-binding sites of a variety of glycoses have been gained by NMR investigations on boron and molybdenum complexes.^[4] However, firm knowledge in terms of both crystal-structure work and NMR spectroscopy in solution has remained elusive. Presently, this criterion is met by only two classes of glucose complexes, one of which comprises a series of aldose-palladium(II) complexes in aqueous solu-

[a] X. Kästele, Prof. Dr. P. Klüfers, Dipl.-Chem. F. Kopp, Dr. J. Schuhmacher, Dr. M. Vogt
Department Chemie und Biochemie der Ludwig-Maximilians Universität
Butenandtstrasse 5–13, 81377 München (Germany)
Fax: (+49)89-2180-77407
E-mail: kluef@cup.uni-muenchen.de

[**] Polyol Metal Complexes, Part 51. For Part 50 see: A. Geißelmann, P. Klüfers, C. Kropfgans, P. Mayer, H. Piotrowski, *Angew. Chem.* **2005**, *117*, 946–949; *Angew. Chem. Int. Ed.* **2005**, *44*, 924–927.

Supporting information for this article is available on the WWW under <http://www.chemeurj.org/> or from the author.

tion, with the second containing a number of glucose-phenylsilicates in methanolic solution and includes some aldopentoses as well as two ketoses.^[5-7] From the viewpoint of the carbohydrate, palladium is a “conservative” bonding partner as bonding to palladium alters the equilibrium mixture of aldose isomers in only a limited way—the prevalence of the pyranoses is maintained on deprotonation and bonding by the rather large metal center.^[5,6] Silicon binding, on the other hand, induces a radical shift of the isomer mixture in the protic methanol solvent towards the furanose that bears its anomeric hydroxy group *cis* to the epimeric one. Thus, the most acidic *cis*-furanose group of a monosaccharide acts as a bidentate silicon chelator in the isolated bis-(diolato)(phenyl)silicates, as shown in the synthetic strategy that has been derived from studies on glucose model compounds.^[7]

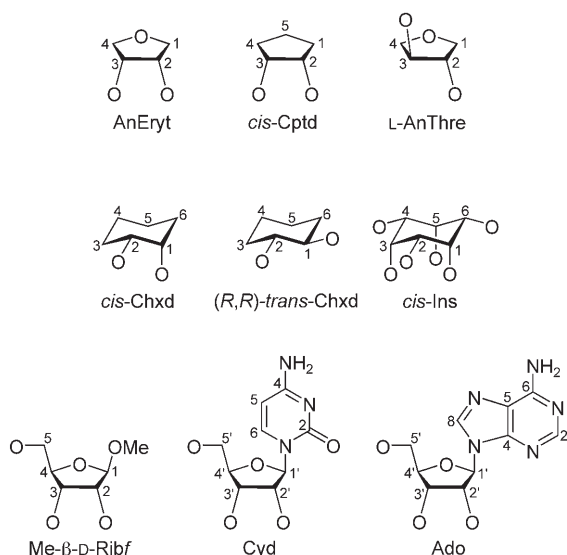
To master the difficulties of the conformationally unstable and polyfunctional glucose ligands in a rational way, carbohydrate model compounds that provide isolated binding sites are a prerequisite for evaluating the metal-binding sites in question. The simpler such compounds are, however, the less representative they are as carbohydrate models. Hence the diol function of a carbohydrate is badly modeled, for example, by ethylene glycol (1,2-dihydroxyethane), which resembles the diol function(s) of a sugar neither in terms of acidity nor in terms of steric restrictions. In this situation, anhydroerythritol (*cis*-oxolane-3,4-diol, abbr.: AnEryt, Scheme 1) is an optimum “in-between” molecule as, on the one hand, AnEryt is closely related to the carbohydrates as it can be considered to be a molecular cut-out of such important glycosides as the nucleosides (Scheme 1), and, moreover, its acidity is about the same as that of the glycosides, including the polysaccharides.^[8] On the other hand, AnEryt is easily obtainable, configurationally stable in the entire pH

range of interest, and chemically stable under alkaline conditions. AnEryt shares the latter two properties, which are critical for the glycosides, with the glycosides. Contrary to even glycosides, AnEryt is achiral, a property that we found to be beneficial for the crystallization of its complexes. Finally, as a *meso* compound, AnEryt gives rise to particularly simple ¹³C NMR spectra, which often exhibit a typical “coordination-induced shift” (CIS), usually a downfield shift of the signals of those carbons that bear metal-binding oxygen atoms. These properties have led to extensive use of AnEryt as a bridge to carbohydrate-(semi)metal chemistry, both in the area of transition-metal as well as in main-group chemistry.

The fact that AnEryt models a furanoside and not a pyranoside is of particular importance if one is dealing with small central atoms. For silicon, it has been shown that no complexes are formed in aqueous media upon reaction with *trans*-pyranoidic diol moieties. Instead, hydrogen-bonded oligosilicate-oligosaccharide assemblies can be isolated, as has been shown for α -cyclodextrin as the carbohydrate component.^[9] Contrary to *trans*-pyranoidic diols, silicon-chelating properties have been found with sugar alcohols—glyconic and glycaric acids—whose open-chain diol groups are more flexible.^[10] However, to open the way to a diolatosilicate chemistry in aqueous solution for a sugar alcohol, support by a pattern of spatially suited hydrogen bonds is required.^[11] *cis*-Furanoidic diols like AnEryt, but also the ribofuranosides, including the nucleosides and the furanoses, intrinsically provide the property of silicon chelation in aqueous media without the need for support by secondary interactions such as hydrogen bonds.

For these reasons, AnEryt plays a leading role in the rapidly growing field of the carbohydrate chemistry of silicon: the first hydrolytically stable Si–O–C linkage was prepared with AnEryt.^[12] The privileged position of furanoidic diols as silicon chelators has been derived by comparing AnEryt and open-chain polyols.^[11] NMR work by Kinrade et al. concerning the question of isomers at pentacoordinate silicon centers has focused on AnEryt,^[13] and the latest published work concerns the attempts of Lambert et al. to use ¹³C NMR shift differences derived from AnEryt-silicate solutions as the key to aqueous glucose-silicate chemistry.^[14] In this work, an unusual number of misleading errors accumulate, and these are discussed in some detail in the Supporting Information. Most of them originate in an uncritical application of shift-difference concepts. Thus, as a methodological leitmotif, the NMR spectroscopic properties of the respective compound classes are deduced here in order to provide reliable data in particular on shift-difference rules, which are a valuable tool when applied carefully.

The chemical focus of the present work is the astonishingly multifaceted silicon chemistry of AnEryt. On the one hand, AnEryt is a powerful tool for surmounting the obstacles of carbohydrate-silicon chemistry but, on the other, and like its carba analog *cis*-cyclopentanediol, AnEryt exhibits a unique and unexpected alkoxy silane chemistry which appears to be untransferable to a polyfunctional carbohydrate.



Scheme 1. Diols referred to in this work (hydroxyl hydrogen atoms omitted), including the atomic numbering scheme; AnEryt numbering is derived from the parent polyol erythritol, not from oxolane numbering.

Results

Furanoses—better ligands for silicon: Structural analyses that show five-membered chelate rings of the SiO_2C_2 type always reveal small torsion angles of the O-C-C-O moiety. This finding is to be expected for the C_2O_2 units of, say, catecholate or oxalate,^[15] but is also the case for diolates and the dianions of hydroxycarboxylic acids. In turn, the more cheaply an approximately 0° torsion can be achieved in terms of energy, the better silicon chelators are the diolate ligands derived from carbohydrates. A *cis*-furanoidic diol, that is, a diol group attached *cis* to an oxolane ring, thus appears to be a better choice than open-chain diols and, particularly, pyranoidic diol functions. The reason for the conformational flexibility of a furanose ring is its balance of strain. While open-chain diols experience Pitzer strain when twisted into an eclipsed conformation, and pyranoses are burdened with ring strain on being twisted towards 0° torsion, a furanose is characterized by a balance of the various types of strain over a pronounced range of torsions.

To give an impression of numbers, the torsional energies of some molecules that are related to the carbohydrates have been calculated at the B3LYP/6-31G(d) level of theory. To prevent, in terms of X-ray structures, irrelevant intramolecular hydrogen bonding within the diol group, the hydroxy groups were replaced by fluorine atoms in the calculations. Figure 1 shows the energetic costs for reaching the range of torsion angles of less than about 30° that appears to be typical for silicon–diol bonding. As a result, *trans*-pyranoses (Figure 1 bottom: the perfluoro derivative of β -D-

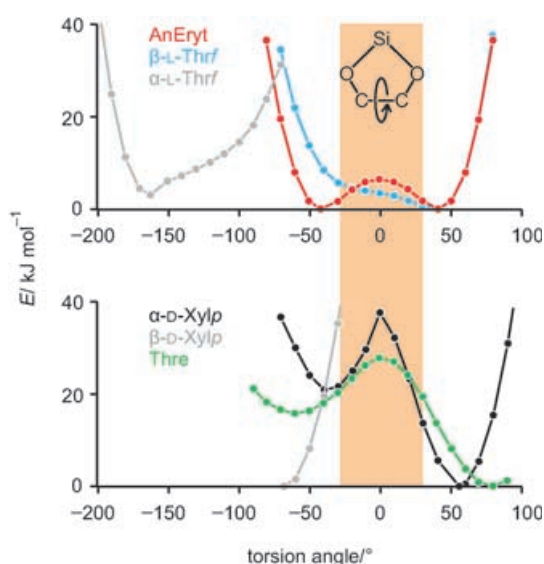


Figure 1. Top: B3LYP/6-31G(d) torsion energies of various F-C-C-F functions in the perfluoro derivatives of α - and β -L-threofuranose (torque about the C1–C2 bond), and anhydroerythritol (torque about the C2–C3 bond). Bottom: B3LYP/6-31G(d) torsion energies of various F-C-C-F functions in the perfluoro derivatives of α - and β -D-xylopyranose (torque about the C1–C2 bond), and D-threitol (torque about the C2–C3 bond). The colored area indicates the range of abscissa values that is spanned in silicon-bonded diols.

xylopyranose) are ruled out as efficient silicon chelators in view of the high energy needed for torsion, in line with the results in the α -cyclodextrin/silicate system mentioned above. As expected, the same result is obtained for *trans*-furanoses: although comprising a much larger range of flexibility at low energy, 0° torsion is far outside the energetically accessible region (Figure 1 top: the perfluoro derivative of α -L-threofuranose). Torsion of a *cis*-pyranose proceeds with less resistance on a path that connects the starting 4C_1 chair and the ${}^4B^1$ boat conformation. In terms of energy, however, *cis*-pyranose (Figure 1 bottom: the perfluoro derivative of α -D-xylopyranose) and open-chain (Figure 1 bottom: the perfluoro derivative of threitol) torsions are significantly more expensive, in energy terms, than torsion of a *cis*-furanoidic molecule (Figure 1 top: the perfluoro derivatives of β -L-threofuranose and anhydroerythritol). For the latter, the typical large range of low-energy conformations of about 100° for furanose includes the 0° point.

To derive the rules of glycofuranose ligation, the *cis*-oxolane diols thus appear to be the first choice. Two diols may be considered. To model the most acidic C1/C2 binding site of a furanose, *cis*-2,3-oxolane diol appears suitable, whereas for modelling the *cis*-furanosides, AnEryt may be a good choice. Of these two diols, AnEryt has benefits for practical work in terms of stability, particularly in alkaline solution (2,3-oxolane diol is much more reactive as it is the hemiacetal of 2,4-dihydroxybutanal).

The applicability of the model calculations on fluorine compounds to the oxo compounds of interest has been proven for some AnEryt conformations. The structures of two AnEryt and one AnEryt·3H₂O conformations were refined at the same level of theory. The O-C-C-O torsion angles are in the range of 30 – 40° , depending on the actual conformation, and include the F-C1-C2-F angle of the fluoro derivative of α -threose of 39.1° . About the same torsion angle, 41.4° , is obtained for the minimum structure of the difluoro derivative of AnEryt. These calculated values are in agreement with the four angles found in the X-ray crystal structures: 40.1° and 41.0° in AnEryt·NaClO₄,^[16] and $38.1(2)^\circ$ and $42.0(2)^\circ$ in two symmetrically independent molecules in the structure of pure AnEryt (Figure 2, left). As a result of both computational and X-ray methods it may therefore be stated that AnEryt does not reside at 0° torsion

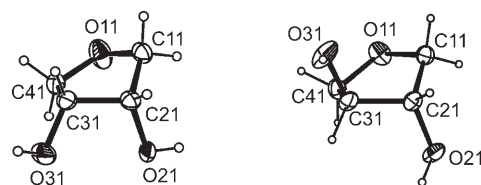


Figure 2. ORTEP diagrams (50% probability ellipsoids) of the two oxolane diols. Left: one of the two symmetrically independent molecules in crystals of AnEryt. The diol torsion angle is $38.1(2)^\circ$ in the depicted molecule (the other value is $42.0(2)^\circ$). Right: one of the three symmetrically independent molecules in crystals of L-AnThre. The diol torsion angle is $166.7(2)^\circ$ in the depicted molecule (the other values are $166.9(2)^\circ$ and $167.2(2)^\circ$).

in its stable conformation, but 0° torsion is available at low cost.

The conformers of the *trans* isomer anhydrothreitol (AnThre) exhibit much larger diol torsion angles in the solid state. The respective mean angle of the L enantiomer (Figure 2, right) is 166.9° , and is also close to the F-C1-C2-F angle in the DFT structure of the fluoro derivative of β -L-threose at minimum energy (162.2°). Keeping in mind the respective curve in Figure 1, chelation of any central atom by a *trans*-furanose, an example being the 1,2-site of β -ribofuranose, is clearly ruled out.

Owing to the repeatedly incorrect assignment of the ^{13}C NMR signals of AnEryt in recent work,^[13,14] let us recall the well-known fact that AnEryt, as opposed to AnThre, exhibits an irregular order of its ^{13}C NMR signals, with C1/C4 being downfield of C2/C3 in the usual solvents (Table 1).^[17]

Table 1. Signal order in the ^{13}C NMR spectra of AnEryt ($c=0.6\text{ mol L}^{-1}$) in various solvents. $\Delta\delta = \delta(\text{C1/C4}) - \delta(\text{C2/C3})$.

	$\delta(\text{C1/C4})$	$\delta(\text{C2/C3})$	$\Delta\delta$
CDCl_3	72.9	71.4	1.5
CD_3OD	73.3	72.5	0.8
1 M [K([18]crown-6)]OMe/MeOH	72.5	71.1	1.4
D_2O	72.9	71.4	1.5

In D_2O , the C1/C4 position is 1.5 ppm downfield of C2/C3, a result that can be rationalized by DFT calculations. At the PBE1PBE/6-311++G(2d,p)//B3LYP/6-31G(d) level, the mean signal positions of the AnEryt-3H₂O aggregate are $\delta = 78.6$ and 77.3 ppm relative to tetramethylsilane for C1/C4 and C2/C3, respectively, and show a 1.3 ppm downfield shift for the carbons adjacent to the diol group, the difference being close to the experimental value for an aqueous solution. It should be mentioned that AnEryt shares this irregularity with some compounds with the AnEryt partial structure. Thus, the C3/C4 signals show a reversed order in the ^{13}C NMR spectra of D-erythrose and the methyl-D-erythrofuransides as well.^[17]

To rationalize the systematic findings derived from computer chemistry, compounds with the diol patterns in question were treated with various silicon-based starting materials to give centers with coordination numbers four, five, and six. The focus of the following sections is on AnEryt, which gives rise to the most widespread chemistry.

Tetracoordinate silicon centers—oxysilanes derived from furanoidic diols: Penta- and hexacoordination of silicon towards polyols is consistently prevented by introducing two organyl substituents at the silicon atom. To examine the structures and NMR shift differences for tetracoordinate silicon centers, the diphenylsilylene moiety was bonded to various diols.

1,2-Cyclohexylenedioxy(diphenyl)silanes: Diol functions attached to six-membered rings like pyranoses should be unable (*trans*-diols) or hardly able (*cis*-diols) to act as silicon

chelators according to the DFT treatment above. This finding was supported by experiments in nonaqueous media, where silicon bonding to such a diol can be forced due to the absence of thermodynamic traps like ortho-silicate. Thus, the *cis* and *trans* isomers of cyclohexane-1,2-diol (Chxd) react with dichlorodiphenylsilane in aprotic media to give products of the net formula $\text{Ph}_2\text{Si}(\text{ChxdH}_{-2})$. The ^{29}Si NMR solution spectra show a single resonance for both diols. The actual values are those for unstrained tetrahedral coordination of the central atom: $\delta = -34.4$ and -35.3 ppm for $\text{Ph}_2\text{Si}(\text{cis-ChxdH}_{-2})$ (**1**) and $\text{Ph}_2\text{Si}(\text{trans-ChxdH}_{-2})$ (**2**) respectively. Crystal-structure analysis revealed the origin of the missing strain: both **1** (Figure 3) and **2** (Figure 4) are in fact dimers. The fact that a single ^{29}Si NMR signal is observed with almost the same value for both isomers can be interpreted in terms of the dimers being the only solution species. Silicon chelation by the *cis*-diol hence does not occur even to a minor extent in the so-

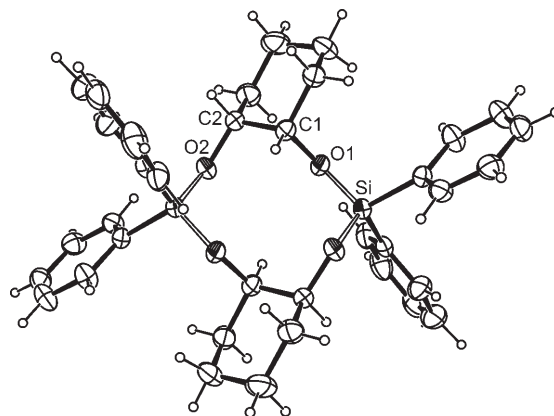


Figure 3. ORTEP diagram (50% probability ellipsoids) of the C_2 -symmetrical dimers in crystals of **1**. Bond lengths [Å] and angles [°]: Si–O1 1.631(1), Si–O2' 1.637(2); O1–Si–O2' 111.97(7); diol torsion: $61.0(2)^\circ$. Symmetry code: $i: 1-x, 1-y, 1-z$.

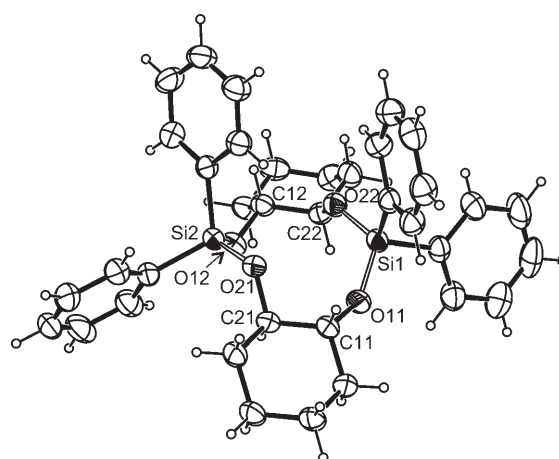


Figure 4. ORTEP diagram (50% probability ellipsoids) of the dimers in crystals of **2**. Bond lengths [Å] and angles [°]: Si1–O11 1.619(1), Si1–O22 1.638(1), Si2–O12 1.634(1), Si2–O21 1.637(1); O11–Si1–O22 114.28(7), O12–Si2–O21 113.57(7); torsion: $-61.1(2)^\circ$ for both diol groups.

lution equilibrium. The chemical shifts and shift differences in the ^{13}C NMR spectra are given in Table 2. It should be noted that shift differences on H/Si exchange are hardly significant for these nonchelated four-coordinate silanes.

Table 2. Chemical shifts in the ^{13}C NMR spectra of the $\text{Ph}_2\text{Si}(\text{ChxdH}_{-2})$ isomers **1** and **2**, and shift differences ($\delta(\mathbf{1/2})-\delta(\text{free diol})$). Bold: $\Delta\delta$ of those carbon atoms that bear the silicon-binding oxygens.

		C1/C2	C3/C6	C4/C5
1	δ [ppm]	77.5	30.4	21.7
	$\Delta\delta$ [ppm]	1.6	0.4	0.2
2	δ [ppm]	76.9	34.1	24.2
	$\Delta\delta$ [ppm]	1.4	1.1	0.2

3,4-Oxolanenedioxy(diphenyl)silanes and 1,2-cyclopentylenedioxy(diphenyl)silane: The structural and spectral properties of four-coordinate Si centers bonded to an alkylenedioxy substituent derived from a furanoidic diol were investigated with the two isomeric oxolane-3,4-diols. Thus, in addition to AnEryt, anhydrothreitol (AnThre) was included in this part of the investigation to demonstrate the inability of furanoidic *trans*-diols to form five-membered chelate rings.

Dichlorodiphenylsilane reacts with AnEryt or L-AnThre in trichloromethane, in the presence of pyridine as a base, to form $\text{Ph}_2\text{Si}(\text{AnErytH}_{-2})$ (**3**) and $\text{Ph}_2\text{Si}(\text{L-AnThreH}_{-2})$ (**4**), respectively. The crystal structure of **3** is shown in Figure 5.

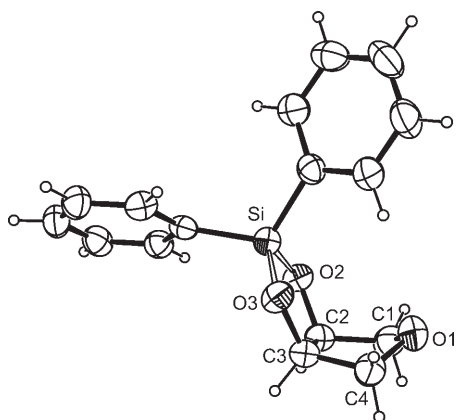


Figure 5. ORTEP diagram (50% probability ellipsoids) of one of the two symmetrically independent monomers in crystals of **3**. Bond lengths [Å] and angles [°]: Si1–O21 1.649(2), Si1–O31 1.642(2); O21–Si1–O31 97.9(1); diol torsion: $-5.4(2)$ ($-6.7(2)^\circ$ for the second molecule in the asymmetric unit).

The molecular structure is that of a monomer. Contrary to the case of the cyclohexylenedioxy derivatives, chelation is possible with the furanoidic diol. As expected, the five-membered chelate ring is almost planar, with a diol torsion angle close to 0° . Such geometrical parameters cannot be met by AnThre. However, this diol provides another example that the inability to form a chelate ring must not be confused with a lack of reactivity. Thus, the solid-state structure

of **4** is not that of a monomeric chelate. Instead, an unstrained molecule with all bonding angles close to their ideal values is observed in a trimeric structure (Figure 6). Although 0° torsion is outside the range of achievable diol torsion angles, the great flexibility of furanoidic rings is obvious from the AnThre structure as well. To build up the trimer, the diol torsion angles almost span the entire available 100° range of a furanoidic diol, with the actual values being between 82° and 165° .

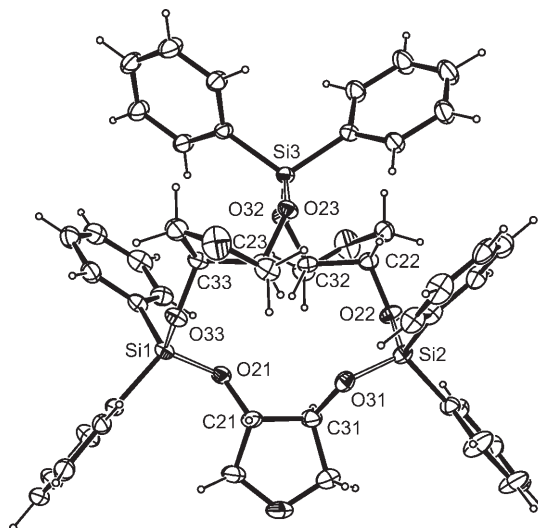


Figure 6. ORTEP diagram (50% probability ellipsoids) of the C_1 -symmetrical trimers in crystals of **4**. Mean bond lengths [Å] and angles [°]: Si–O 1.638; O–Si–O 112.1. Diol torsion $\text{O}2n\text{-C}2n\text{-C}3n\text{-O}3n$: $81.6(4)^\circ$ for $n=1$, $164.6(2)^\circ$ for $n=2$, and $163.3(2)^\circ$ for $n=3$.

The ^{29}Si NMR spectra verify the assumption that the molecules found in the solid state are also the solution species. Thus, a single resonance is observed for solutions of both oxolanediols. The value for **4** ($\delta = -29.6$ ppm) resembles the value for the also unstrained but dimeric (cyclohexylenedioxy)silanes. The AnEryt derivative, however, shows a distinct downfield shift ($\delta = -1.4$ ppm). The ^{13}C NMR spectra of the same solutions exhibit larger shift-differences for H/Si exchange than the Chxd derivatives. For the chelating silane, the numerical values in Table 3 show that the ^{13}C NMR signals of those carbon atoms that bear the sili-

Table 3. Chemical shifts in the ^{13}C NMR spectra of $\text{Ph}_2\text{Si}(\text{DiolH}_{-2})$ derived from diols attached to five-membered rings, and shift differences ($\delta(\text{Si-bonded})-\delta(\text{free diol})$). Bold: $\Delta\delta$ of those carbon atoms that bear the silicon-binding oxygens. The atomic numbering of the cyclopentane-diol has been adapted to the oxolanediols (cf. Scheme 1).

		C2/C3	C1/C4	C5
5	δ [ppm]	80.1	35.2	22.5
	$\Delta\delta$ [ppm]	7.2	4.3	2.7
3	δ [ppm]	79.2	75.2	
	$\Delta\delta$ [ppm]	7.8	2.3	
4	δ [ppm]	80.0	73.0	
	$\Delta\delta$ [ppm]	3.7	0.0	

con-binding oxygens are shifted downfield by almost 8 ppm. However, mere H/Si exchange is obviously not the only factor responsible for this significant shift difference, as is shown by the AnThre values, which are about half of the AnEryt values even though the structures are isomeric.

The body of shift-difference data was enlarged by investigating the carba analog of AnEryt, namely *cis*-cyclopentane-1,2-diol (*cis*-Cptd). The usual synthetic procedure yielded solutions of $\text{Ph}_2\text{Si}(\text{cis-CptdH}_2)$ (**5**), which contain monomeric molecules according to the ^{29}Si NMR spectra ($\delta = -3.7$ ppm). The ^{13}C NMR spectroscopic data verify the assumption of monomeric molecules in solution as well, as the shift differences closely resemble the high values of the AnEryt case and not those of the AnThre-derived trimer (Table 3). On crystallization, however, a significant change of the ^{29}Si NMR spectrum was observed. In the solid, the respective signal is shifted more than 30 ppm upfield. The molecular origin of this large shift difference was unraveled by an X-ray analysis (Figure 7): dimerization has occurred and

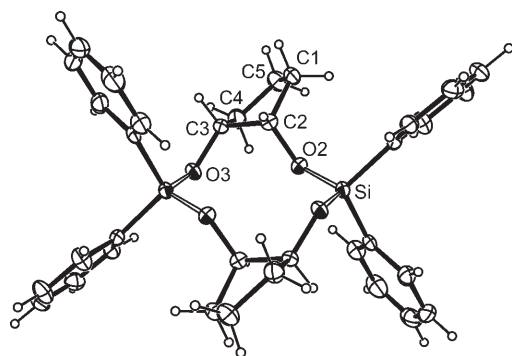


Figure 7. ORTEP diagram (50% probability ellipsoids) of the C_2 -symmetrical dimers in crystals of **5**. Bond lengths [\AA] and angles [$^\circ$]: Si–O2 1.629(1), Si1–O3' 1.636(2); O2–Si–O3' 112.51(8) $^\circ$; diol torsion: 52.4(2) $^\circ$. Symmetry code: i : 1– x , 1– y , 1– z .

an unstrained structure with bonding angles at the Si center close to the tetrahedral angle has formed. Thus, even a diol group attached to a five-membered ring, which is capable of chelating a silicon atom in principle, is obviously able to support the formation of unstrained oligomers as well.

The data in the preceding section stress the fact that in ^{13}C NMR spectra a substantial downfield shift occurs on H/Si exchange provided the discussion is restricted to chelating silanes.

Bis(cycloalkylenedioxy)silanes derived from anhydroerythritol or cis-cyclopentane-1,2-diol: As the next step towards carbohydrate–silicate complexation, the steric and electronic restrictions introduced by the two organyl substituents were lifted. Starting with SiCl_4 as an organyl-free silicon source, the acyclic diol pinacol (2,3-dimethylbutane-2,3-diol) forms a spirocyclic bis(alkylenedioxy)silane.^[18] Furanoidic diols, however, were not used in this context. Since not many data on such compounds are available, both AnEryt and its carba analog *cis*-Cptd were also included in this part of the investigation.

Tetrachlorosilane and a double molar amount of either AnEryt or *cis*-Cptd react, upon heating in toluene, with formation of hydrogen chloride. The ^{29}Si and ^{13}C NMR spectra indicate formation of the expected spiro compounds. For both diols, the ^{13}C NMR signals are doubled according to the spiro pattern and are shifted downfield. In the case of AnEryt, the downfield shift in toluene solution roughly resembles that of the analogous diphenylsilane ($\Delta\delta = 6.2$ and 6.3 ppm for C2/C3, and 2.0 and 2.1 ppm for C1/C4; ^{29}Si NMR: $\delta = -36.7$ ppm). The respective ^{13}C NMR values for *cis*-Cptd are shifted to a smaller extent ($\Delta\delta = 3.5$ and 3.7 ppm for C1/2, 2.0 and 2.2 ppm for C3/5, and 0.9 for C4; ^{29}Si : $\delta = -36.8$ ppm). The ^{29}Si NMR spectroscopic data, which are typical for strained chelate rings, again show a pronounced downfield shift when compared to an unstrained $\text{Si}(\text{OR})_4$ reference like tetramethoxysilane ($\delta = -78.0$ ppm).

Attempts to crystallize the silicic acid ester of anhydroerythritol yielded a total of four polymorphic forms of $\text{Si}(\text{AnErytH}_2)_2$ (**6**). When sorted according to the molecular structures, three polymorphs are formed from the spirocyclic molecules whose synthesis had been attempted. The trimorphic spirosilane is termed α -**6**, β -**6**, and γ -**6** according to decreasing density. The molecular structure of α -**6**, which is depicted in Figure 8, is representative of all the modifications

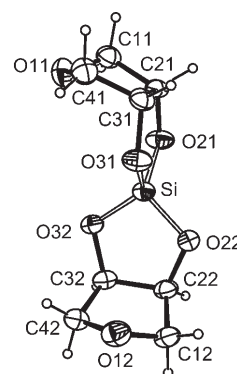


Figure 8. ORTEP diagram (50% probability ellipsoids) of the monomeric spirosilane in crystals of α -**6**. Bond lengths [\AA] and angles [$^\circ$]: Si–O21 1.628(2), Si–O22 1.629(2), Si–O31 1.619(2), Si–O32 1.625(1); O21–Si–O31 99.05(9), O22–Si–O32 98.73(7); diol torsion: O21–C21–C31–O31: $-0.8(2)^\circ$; O22–C22–C32–O32: $-1.2(2)^\circ$.

of **6**. The common features include, again, almost flat SiO_2C_2 chelate rings with approximately zero torsion of the oxolanylenedioxy moiety (i.e. almost ideal local D_{2d} symmetry of the silacycles), and bending of the oxolane O-atoms towards the silicon atom. Although the differences with respect to molecular symmetry are small, the packing patterns of the molecules are completely different in the polymorphs. Hence, no group–subgroup relationships connect the polymorphs nor are there phase transitions between the monomer forms on heating. Thermal analysis, optical inspection on heating, and X-ray powder diffraction at various temperatures show partial melting and re-solidifying until eventual-

ly all the samples melt at the melting point of β -6. On cooling, the melts solidify uniformly to yield only β -6.

This latter property has also been found in a fourth polymorph, whose crystallization follows a special protocol: crystallization from toluene solutions succeeded at about 4°C after the solutions were saturated at the same temperature with respect to the fourth polymorph (i.e., saturate at room temp., crystallize at 4°C for about four days, remove crystals of α -6 completely, and allow the solution to stand at 4°C for a further 2–3 weeks). ^{29}Si solid-state NMR spectra indicate that the molecular structure of this polymorph is different ($\delta = -36.7$, -37.9 , and -36.6 ppm for α -, β -, and γ -6, respectively; $\delta = -94.3$ ppm for the fourth polymorph). X-ray analysis revealed an unexpected molecular structure. As shown in Figure 9, the crystals are made up of dimers of the spiro-

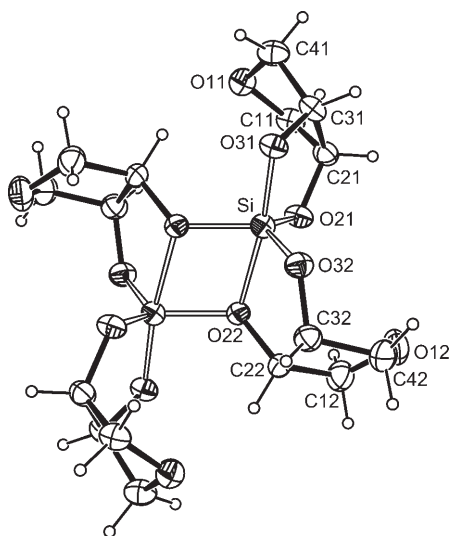


Figure 9. ORTEP diagram (50% probability ellipsoids) of the C_2 -symmetrical dimers in crystals of $\text{Si}(\text{AnErytH}_2)_2$. Bond lengths [Å]: Si–O21 1.650(2), Si–O22 1.929(2), Si–O22' 1.732(2), Si–O31 1.667(2), Si–O32 1.641(2); diol torsion: O21–C21–C31–O31: $-2.8(3)^\circ$; O22–C22–C32–O32: $-16.8(3)^\circ$. Symmetry code: $i: 1-x, 1-y, 1-z$.

lane but not of the tetracoordinate type, whose formation might be plausible as a means of reducing steric strain in the chelate rings as with **5**. Instead, the coordination number of silicon is five, which is not unusual for anionic Si centers but is a new and unexpected structural motif for a simple silicic acid ester.

When AnEryt is replaced by its carba analogue *cis*-Cptd, the solutions of the monomeric spirosilane show a different crystallization behavior, as monitored by ^{29}Si solid-state NMR spectroscopy. Under various crystallization conditions, the Cptd ester always shows downfield-shifted resonances typical for pentacoordination. Thus, an approximate 60 ppm shift difference of the ^{29}Si NMR signal is obtained for gently ground crystals of $\text{Si}(\text{CptdH}_2)_2$ (**7**) that had been grown from a toluene solution (solid state: $\delta = -94.7$ ppm; solution: $\delta = -36.8$ ppm). Gentle grinding is essential to record the solid-state signal correctly due to the mechanical sensi-

tivity of the substance. After thorough grinding, the main signal is observed at $\delta = -80$ ppm, which is indicative of unstrained tetrahedral $\text{Si}(\text{OR})_4$ coordination at silicon (cf. the $\delta = -78$ ppm signal of tetramethoxysilane) in a tentative oligomer or polymer. Attempts to grow crystals of the monomer failed; even sublimation yielded a dimer instead of a monomer according to solid-state ^{29}Si NMR spectroscopy ($\delta = -94.6$ ppm). A structure analysis confirmed a second modification of the dimeric pentacoordinate Cptd ester. The molecular structures of the two modifications are very similar, hence only the structure of β -7₂ (crystals grown from toluene) is depicted in Figure 10.

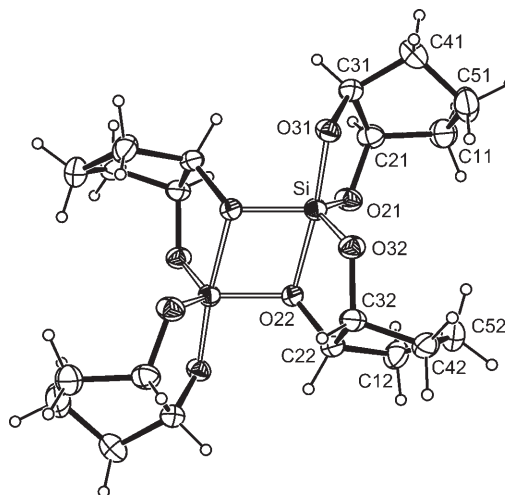


Figure 10. ORTEP diagram (50% probability ellipsoids) of the C_2 -symmetrical dimers in crystals of β -7₂. Bond lengths [Å]: Si–O21 1.651(2), Si–O22 1.929(1), Si–O22' 1.726(1), Si–O31 1.672(1), Si–O32 1.641(2); diol torsion: O21–C21–C31–O31: $11.8(2)^\circ$; O22–C22–C32–O32: $-27.3(2)^\circ$. Symmetry code: $i: -x, -y, -z$.

The structures of the Si_2O_8 cores of **6**₂ and **7**₂ are the same. Two Si–O distances are substantially longer than the other ones, although these longer Si–O bonds are not the new bonds that are formed on dimerization. Thus, the new structures appear to be stabilized transition states of dimerization towards molecules like **5**₂. Such aspects were investigated by DFT methods. These results, which include the close resemblance of calculated and solid-state structures, the almost equal energy of a pair of monomers and the respective dimer, and the low activation energy for formation and cleavage of the dimer, will be published in a separate paper. Although the focus of this work lies in a critical evaluation of NMR shift differences in the diol/silicon field, the solid-state structures of **6**₂ and **7**₂ show that the chemistry of simple model diols is not free of surprising results, thus indicating that not only the carbohydrate–silicon interaction is waiting to be uncovered, but also the basic chemistry behind it.

What about the typical shift differences in the NMR spectra? Having arrived at this point, things seem to develop promisingly. Chelation—not mere binding—of tetracoordinate silicon centers by alkylendioxy groups is indicated

both by a typical downfield shift in the ^{29}Si NMR spectra and by a typical coordination-induced shift in the ^{13}C NMR spectra of 6–8 ppm downfield. Note, however, the lower values for **7**.

Pentacoordinate silicates with AnErytH₂ ligands

Structures of the alkali-metal salts of the [Si(OH)(AnErytH₂)₂]⁻ ion: The current focus of the discussion is doubtless the aqueous chemistry of the silicate/AnEryt system. When introducing water as the solvent, protolytic and hydrolytic equilibria have to be considered in addition to the chelation/oligomerization chemistry discussed above. Thus, hydrolysis of the spirocyclic silane Si(AnErytH₂)₂ in neutral or acidic aqueous solution may start by the addition of a water molecule to form a transient pentacoordinate species [Si(H₂O)(AnErytH₂)₂]. At higher pH, the mono-deprotonated anion of this hypothetical acid is the predominant species, which is obtained directly by the action of AnEryt on silica in alkali lye.

As discussed both in Lambert's work and in a work of the Kinrade group, such aqueous solutions show three signals in the ^{29}Si NMR spectra in the region of pentacoordinate silicon.^[13,14] Thus, the question of isomerism arises. To get an idea of what kinds of isomers have to be considered for these pentacoordinate silicates, a look at solid-state structures is helpful. Presently, a total of five crystal structures are available. In addition to the published structures of Li[Si(OH)(AnErytH₂)₂]·H₂O and K[Si(OH)(AnErytH₂)₂],^[12] the anhydrous Na, Rb, and Cs salts have been crystallized from aqueous solutions and structurally resolved by single-crystal X-ray analysis. The structure of the silicate ion in Na[Si(OH)(AnErytH₂)₂] (**8a**) is shown in Figure 11. In a

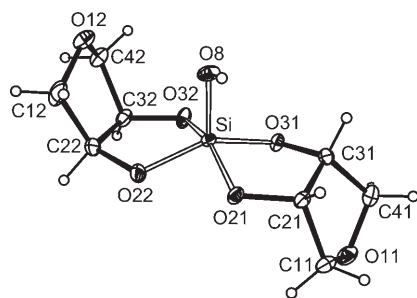


Figure 11. ORTEP diagram (50% probability ellipsoids) of the anions in crystals of **8a**. Bond lengths [Å]: Si–O21 1.730(2), Si–O22 1.734(2), Si–O31 1.728(2), Si–O32 1.720(2), Si–O8 1.662(2); diol torsion: O21–C21–C31–O31: 14.1(2)°; O22–C22–C32–O32: 9.7(2)°.

slightly distorted square-pyramidal (sp) coordination at the silicon center, the hydroxo ligand takes the apical position. Each diolate is bonded in the basal plane, which is the only possible position since the “bite” of a diolate ligand is not large enough to span a basal/apical chelate with its larger angle at silicon. Two different orientations are taken by the oxolane rings. One of them is located on the same face of the corresponding chelate ring as the hydroxo ligand (*syn*),

whereas the other oxolane ring and the hydroxo ligand are on different faces of the respective chelate ring (*anti*). As for the lithium and potassium analogs, the sodium compound contains both *syn* and *anti* isomers. Another structural motif is found in the isotopic Rb (**8b**) and Cs (**8c**) salts. The anion structure of the Cs salt **8c** is shown in Figure 12.

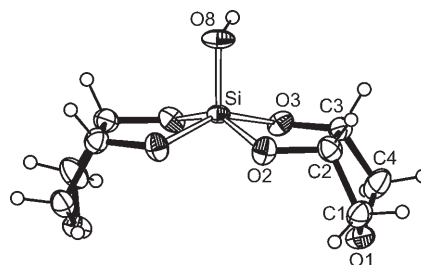


Figure 12. ORTEP diagram (40% probability ellipsoids) of the C₂-symmetrical anions in crystals of **8c**. Bond lengths [Å]: Si–O2 1.730(4), Si–O3 1.720(3), Si–O8 1.652(5); diol torsion (O2–C2–C3–O3): –3.5(5)°.

With these larger cations the *anti/anti* isomer is isolated, with the coordination at silicon being sp as with the lithium and sodium salt. The only exception to sp coordination is found with potassium as the counterion. The hydroxo ligand takes an equatorial position in this case, and each diolate ligand is bonded axially/equatorially, which is the only possible position since, again, the bite of a diolate ligand is too small to span an equatorial/equatorial chelate. Table 4 gives a comprehensive survey of significant data on the five alkali-metal diolatosilicates.

Table 4. Solid-state properties of the pentacoordinate silicates A[Si(OH)(AnErytH₂)₂] (A = Li–Cs; the Li salt crystallizes as a monohydrate). Reference denotes the work where the structure is described; all NMR spectroscopic data are from this work.

A	Isomer ^[a]	Si ^[b]	% tbp ^[c]	^{29}Si ^[d]	Reference
Li	<i>syn/anti</i>	sp	2.0	–95.5	[12]
Na	<i>syn/anti</i>	sp	7.8	–97.6	this work
K	<i>syn/anti</i>	tbp	62.7	–98.3	[14]
Rb	<i>anti/anti</i>	sp	13.9	–92.7	this work
Cs	<i>anti/anti</i>	sp	13.3	–92.9	this work

[a] Orientation of the oxolane ring relative to the hydroxy ligand. [b] Coordination at Si. [c] Percentage distortion of sp towards tbp (cf. R. R. Holmes, *Prog. Inorg. Chem.* **1984**, 32, 119–235). [d] Solid-state ^{29}Si NMR chemical shift.

As a result, two kinds of isomers have to be considered at the pentacoordinate silicon centers: *syn/anti* and sp/tbp. Prior to a search for such isomers in solution by NMR spectroscopy, it would be helpful to have an idea what activation barriers may be expected for the mutual transformation of such isomers in order to decide whether these isomers can be expected to be resolved on the NMR time scale. For this purpose, DFT calculations were performed on the isolated [Si(OH)(AnErytH₂)₂]⁻ ion, not for modeling the reaction path for *syn/anti* isomerization, which surely cannot be de-

scribed in a realistic way by considering the isolated anion only, but to learn about *sp*/*tbp* isomerism.

The question was dealt with using an overall *anti/anti* geometry first. At the B3LYP/6-31G(d) level of theory for structure optimization, the *sp* structure found in the crystalline state refined to minimum energy on changing to *tbp*, whereas starting with overall *syn/anti* geometry and *sp* coordination at silicon, a local minimum structure of *sp* geometry is only achieved if a hydrogen bond from the hydroxo ligand as the donor towards the oxolane O-atom of the *syn* substituent is provided in the starting geometry. Directing the O-H vector away from the ether oxygen results in a transformation of the starting *sp* geometry to the *tbp* structure. When starting the refinement of a *tbp* structure with the hydrogen bond towards the oxolane-O acceptor, this bond is destroyed in favor of a bond to one of the alkoxy O-atoms. From this refinement behavior, we conclude that no considerable activation barriers should exist between the *sp* and *tbp* forms of the anion in question. *sp*/*tbp* Isomerism thus should not be detectable in real-world experiments, thus leaving *syn/anti* isomerism as the only type of isomerism to be considered. It should be recalled at this point that in the crystalline alkali-metal salts only the *syn/anti* and the *anti/anti* geometries have been found. The *syn/syn* case has never been observed in solid-state work, despite both Lambert and Kinrade's discovery of this geometry in a work by our group which, however, does not deal with silicates at all.^[12-14] As a result of this section, the interpretation of the three signals in the ²⁹Si NMR solution spectra in terms of *syn/anti* isomerism appears straightforward, in agreement with Lambert's suggestion and Kinrade's revision of his

former oligomerization hypothesis, which was based on the assumption that the *syn/syn* case is the only stable one (see above).^[13,14]

However, transformations at the silicon centers other than *syn/anti* have to be considered. Examples include reactions at the hydroxo ligand such as condensation. Thus, a condensation reaction may yield products like $[(\text{AnErytH}_{-2})_2\text{Si}-\text{O}-\text{Si}(\text{AnErytH}_{-2})_2]^{2-}$, which appear possible in view of related species published by the Tacke group, which has used hydroxycarboxylic acids as ligands.^[19] An experimental hint regarding the occurrence of such condensation comes from thermal analysis of the potassium and cesium compounds. Both salts lose half a mole of water per formula unit at a temperature of 280 °C, and they then decompose without melting at about 400 °C.

To gain deeper insight into the significance of condensation of hydroxo ligands in solution, analogous phenylsilicates of the formula $[\text{SiPh}(\text{AnErytH}_{-2})_2]^-$ were included in the investigation.

The $[\text{SiPh}(\text{AnErytH}_{-2})_2]^-$ ion and its relation to the hydroxo analog: Bis(diolato)(phenyl)silicates were obtained by switching to trimethoxyphenylsilane/methanol instead of silicate/water. When both condensation and hydrolysis are prevented by this modification, *syn/anti* isomers of the $[\text{SiPh}(\text{AnErytH}_{-2})_2]^-$ ion should remain as the only species. The ²⁹Si NMR spectra of such solutions exhibit the signals of two major and one minor pentacoordinate species. The similarity of these spectra to those recorded from aqueous silicate solutions is obvious (Figure 13). In agreement with the existence of two main species, crystallization with potassium as

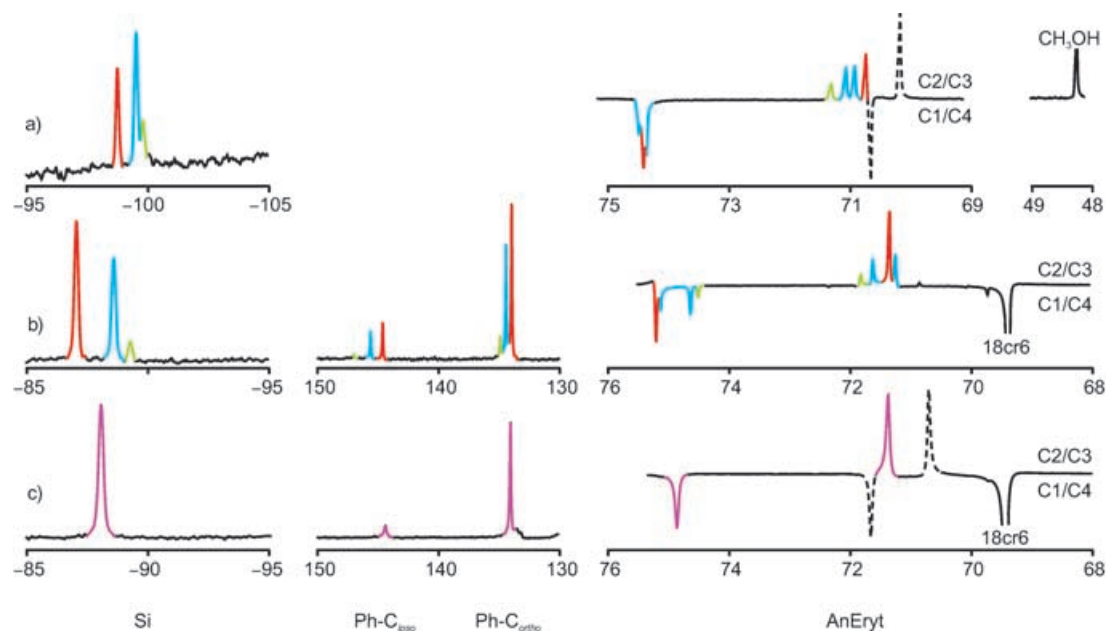


Figure 13. ²⁹Si and ¹³C (DEPT-135) NMR spectra of pentacoordinate AnEryt-silicate species prepared from the diol, SiPh(OMe)₃ or Si(OMe)₄, and base at the molar ratio given in a)–c). Color code: red: *anti/anti*; blue: *syn/anti*; green: *syn/syn* isomer of the respective $[\text{Si}(\text{R})(\text{AnErytH}_{-2})_2]^-$ ion; violet: equilibrating isomer mixture. a) R=OH; base: LiOH; solvent: water; molar ratio: 3:1:1; total Si concentration: 0.54 mol kg⁻¹. The methanol signal stems from hydrolysis of the Si(OMe)₄ starting material and may be used as a reference for DEPT assignment. Dashed line: free AnEryt. b) R=Ph; base: KOMe/[18]crown-6; solvent: methanol; molar ratio: 2:1:2; total Si concentration: 0.38 mol kg⁻¹. AnEryt region in DEPT mode referenced to the [18]crown-6 signal. c) Same as (b), but with a molar ratio of 3:1:1; total Si concentration: 0.61 mol kg⁻¹. Dashed line: free AnEryt.

the counterion yields crystals of the formula $K[\text{SiPh}(\text{AnErytH}_{-2})_2] \cdot 1/2\text{MeOH}$ (**9**) which are made up of the *anti/anti* and the *syn/anti* phenylsilicate in equal parts (Figure 14). Thus, the two main signals in the ^{29}Si NMR

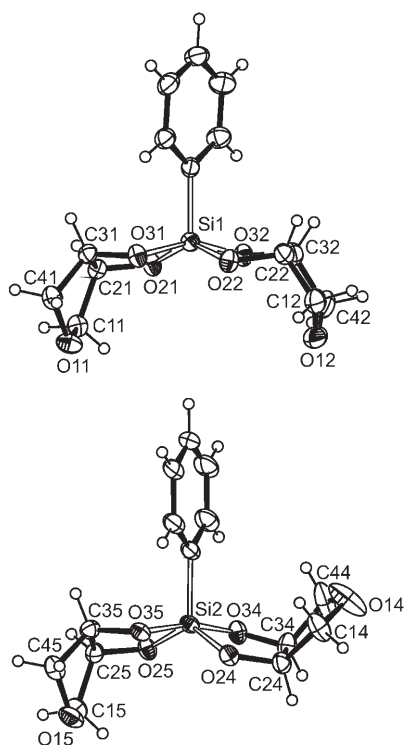


Figure 14. ORTEP diagram (40% probability ellipsoids) of the anions in crystals of $K[\text{SiPh}(\text{AnErytH}_{-2})_2] \cdot 1/2\text{MeOH}$. Distances [Å] in the *anti/anti* isomer (top): Si–O21 1.719(2), Si–O31 1.749(2), Si–O22 1.733(2), Si–O32 1.725(2), Si–C 1.887(3); diol torsion: O21–C21–C31–O31: $-16.4(3)^\circ$; O22–C22–C32–O32: $6.2(3)^\circ$. Distances [Å] in the *syn/anti* isomer (bottom): Si–O24 1.711(2), Si–O34 1.752(2), Si–O25 1.710(2), Si–O35 1.766(2), Si–C 1.899(3); diol torsion: O24–C24–C34–O34: $-3.1(3)^\circ$; O25–C25–C35–O35: $-22.2(3)^\circ$. Percentage distance from the square-planar coordination along the Berry pseudorotation coordinate: *anti/anti* isomer: 23.0; *syn/anti* isomer: 64.5.

spectrum are assigned to the *anti/anti* and the *syn/anti* isomers. In light of this assumption, interpretation of the ^{13}C NMR spectrum is straightforward. Neglecting *sp/tp* isomerism, both the *anti/anti* and the *syn/syn* isomer have apparent C_{2v} symmetry and should thus give rise to one signal for C2/C3 and one signal for C1/C4. The *syn/anti* isomer on the other hand, with its apparent C_s symmetry, will show twice the number of signals, a phenomenon that has been pointed out by Kinrade for the analogous hydroxosilicate.^[13] The ^{13}C DEPT-135 NMR spectrum is shown in Figure 13b. Both the C1/C4 region (consider the [18]crown-6 signal as a reference for DEPT assignment) and the C2/C3 region at higher field show the expected pattern of one strong signal, two signals of medium intensity, and one weak signal for the *anti/anti*, the *syn/anti*, and the *syn/syn* isomer, respectively. A distinct feature that is observed in the spectra of glycosides with the AnEryt partial structure as well may be noted, namely that the *anti/anti* and one of the *syn/anti* sig-

nals are close together; it may be assumed that this *syn/anti* signal stems from the *anti* part of this isomer. The corresponding spectrum of an aqueous diolatosilicate solution is shown in Figure 13a. The C1/C4 region is less structured but the C2/C3 signals again show the pattern of a single strong signal, a pair of signals of about equal intensity, and a single weak resonance, in agreement with Kinrade's finding.^[13] From the isomer distribution in the crystalline salts we assume that the minor component resembles the *syn/syn* isomer in this system also. Moreover, the fact that both the ^{29}Si and the ^{13}C NMR spectra show such a close resemblance leads us to believe that the chemistry of the aqueous system is also adequately described by taking into account *syn/anti* isomers of a mononuclear bis(diolato)hydroxosilicate as the only relevant type of isomerism.

A special feature of the phenylsilicate spectra will gain significance in more complicated cases. Figure 13 shows the ^{13}C NMR signals of the phenyl residue in addition to the diol signals. It should be noted that both the signals stemming from the *ipso*-carbon atom as well as the signals from the two *ortho*-carbon atoms mirror the ^{29}Si NMR spectrum. These signals appear to be as suitable as the silicon nucleus as a probe, and thus provide a tool for resolving an accidental overlap of ^{29}Si NMR signals.

What about characteristic shift differences in the ^{13}C NMR spectra? Figure 13a shows Si-bonded and free AnEryt. The result is opposite to that of the tetracoordinate chelating silanes. The signals of C2/C3—the carbon atoms of the silicon binding site—are shifted about 1 ppm downfield (about 6–8 ppm in chelating oxolanylenedioxysilanes), whereas the signals of the adjacent carbons experience an about 4 ppm downfield shift (about 2 ppm in the respective silanes). The shift differences are thus sensitive to at least the coordination numbers and possibly to the actual structures. It remains to be clarified whether or not these new values are representative of related silicates of the furanoses.

This result may be compared with published work: by erroneously switching the CH and CH_2 coordinate in their DEPT spectrum, the Lambert group has wrongly assigned both the ^{13}C signals of free and Si-bonded AnEryt and thus derived wrong shift differences, which are then the basis for interpreting the spectra of aldoses and ketoses, which are wrongly assigned as well.^[14]

In attempts to record phenylsilicate NMR spectra with excess AnEryt as an internal standard, an interesting observation was made. In the ^{29}Si NMR spectrum (Figure 13c), a single resonance at an intermediate value is found ($\delta = -87.1$ ppm from a 3:1:1 solution of AnEryt, $\text{PhSi}(\text{OMe})_3$, and KOMe/18-crown-6; cf. $\delta = -87.1$ and -88.6 ppm for the stronger signals in Figure 13b, and $\delta = -89.3$ ppm for the weak signal) instead of a triad of signals. Accordingly, the ^{13}C NMR spectrum shows only four signals for AnEryt: two for the free diol and two downfield-shifted signals for Si-bonded AnEryt (Figure 13c). The shift differences in these methanol solutions are slightly smaller than in aqueous solution: 1.6 ppm downfield for Si-bonded C2/C3 and 3.2 ppm

for C1/C4. Upon varying the composition of the solutions, a simple spectrum is always obtained if free AnEryt is detected in the ^{13}C NMR spectrum, whereas split signals are only present if no signals of free AnEryt are visible. We conclude, then, that rapid equilibration of the three silicate isomers occurs in the presence of excess AnEryt. Catalytic amounts of free AnEryt appear to be sufficient since the AnEryt signals themselves are not affected by equilibration; that is, there are not two signals at a medium position, as often observed with diolato-metal complexes of high kinetic lability.

There is a hint that catalysis/inhibition of *syn/anti* isomerization is not only meaningful on the NMR timescale but also drives crystallization. Instead of the solid-state 1:1 mixture of the isomers in **9**, the pure *anti/anti* form is obtained when small amounts of free AnEryt are present in the otherwise unchanged crystallization batches of **9**. The *anti/anti* isomer thus appears to be the thermodynamically most stable one for the specific counterion/silicate combination of **9**. The structure is not presented here, however, because the quality of the crystals is still low.

It should be noted that rapid *syn/anti* equilibration is not observed on the NMR timescale with the pentacoordinate hydroxosilicates, regardless of whether free diol is detected in the spectra.

Extending the anhydroerythritol core—pentacoordinate silicates with β -D-ribofuranosides: One could still hope at this point to recognize the silicon-binding site(s) of a carbohydrate by shift differences in the ^{13}C NMR spectrum. A knowledge of silicon's coordination number appears to be a prerequisite, which is acceptable since ^{29}Si NMR spectroscopy will provide this number. That the signals of the carbons adjacent to the diol function are shifted to a larger extent than the diol carbons may be accepted as well, as long as this is constant behavior at least for AnEryt derivatives. The fact that there is a marked shift at all is a positive aspect that should not be underestimated.

β -D-Ribofuranosides such as methyl- β -D-ribofuranoside (Me- β -D-Ribf) or the nucleosides were then used as probes. Their structures can be derived from that of AnEryt by adding the additional hydroxymethyl and methoxy or nucleobase residue to the oxolane face opposite the diol group so that the diol group does not experience steric hindrance from the additional functional groups. Similar ligand properties should then be expected for AnEryt and the β -D-ribofuranosides. However, some experimental peculiarities of the nucleosides have to be considered: first, they often form precipitates upon preparation of the required 2:1:1 molar ratio of diol, silicon starting material, and base. Second, there is a marked tendency to form hexacoordinate silicates. Both increased solubility in aqueous solution and hexacoordination are effected by large excesses of base, as has been shown by Kinrade for adenosine and guanosine.^[13] The effects of pure pentacoordination are presented for two couples of reaction mixtures that yielded clear solutions with the 2:1:1 molar ratio: trimethoxyphenylsilane or tetrame-

thoxysilane and adenosine in methanol, and trimethoxyphenylsilane/methanol or aqueous silicate and cytidine. With the $\text{Si}(\text{OMe})_4/\text{OMe}^-/\text{MeOH}$ system, a step is inserted between the inert phenylsilicon moiety and the reactive hydroxysilicon function. The synthetic rationale behind the use of methoxysilicates is commented upon in the ribose section below.

Adenosine: Adenosine (Ado) provides the most complete set of spectra, with little overlap of signals, for the study of *syn/anti* isomerism of pentacoordinate bis(diolato)silicon centers. Figure 15 shows the respective spectra, which can be interpreted completely, without leaving signals unassigned, by assuming two major components and one minor species. We assumed by analogy that the minor species is the *syn/syn* isomer, since no stabilization of the *syn/syn* isomer and, at the same time, destabilization of the *anti/anti* species is obvious with adenosine. In light of this assumption, an assignment is straightforward. Table 5 shows the positions of the signals of those carbons that are closest to the diol group. The 1 ppm/4 ppm AnEryt pattern of shift differences for the diol and adjacent carbons obviously cannot be confirmed entirely. The largest shifts are observed for two of the four signals of the anomeric carbon, that is, at one of the two carbons adjacent to the diol group. The signal of the second adjacent carbon, C4, however, is shifted to a lesser extent. Moreover, a large C1' shift difference is observed for only two of the four C1' signals, thus showing nicely that the connectivity contributes to the shift difference but the particular structure in question does so as well. Although the shift differences are thus of less diagnostic use, it should be noted that a signal shows a particularly distinct isomeric splitting if the carbon atom is close to the silicon center. Thus, the signals of all the diol carbons are well resolved into four components.

Attempts to prepare aqueous silicate solutions at the same molar ratio failed. No clear solutions were obtained; instead, precipitates formed.

Cytidine: The reaction of twice the molar amount of cytidine (Cyd) with trimethoxy(phenyl)silane and methoxide in methanol yields exclusively pentacoordinate silicon according to the ^{29}Si NMR spectra, which have a pattern similar to the analogous AnEryt and Ado systems. The minor component of the three is hardly visible due to more-pronounced signal overlap. The signal pattern of the two major species, however, is in agreement with the assumption of a *syn/anti/anti/anti* mixture without rapid exchange. With the exception of signal overlap in the C1'/C5 region at $\delta = 94\text{--}95$ ppm, all the riboside signals can be unambiguously assigned to their respective carbon atoms. The isomeric splitting is shown in Figure 15c. However, a problem occurs regarding the molar ratio of the isomers. Since the *syn/anti:anti/anti* ratio seems to approach 2:1, all strong signals are of approximately equal intensity. Attempts were made to shift the isomeric ratio by altering the solution composition. Thus, replacement of methanol as the solvent by a 1:1 mixture of meth-

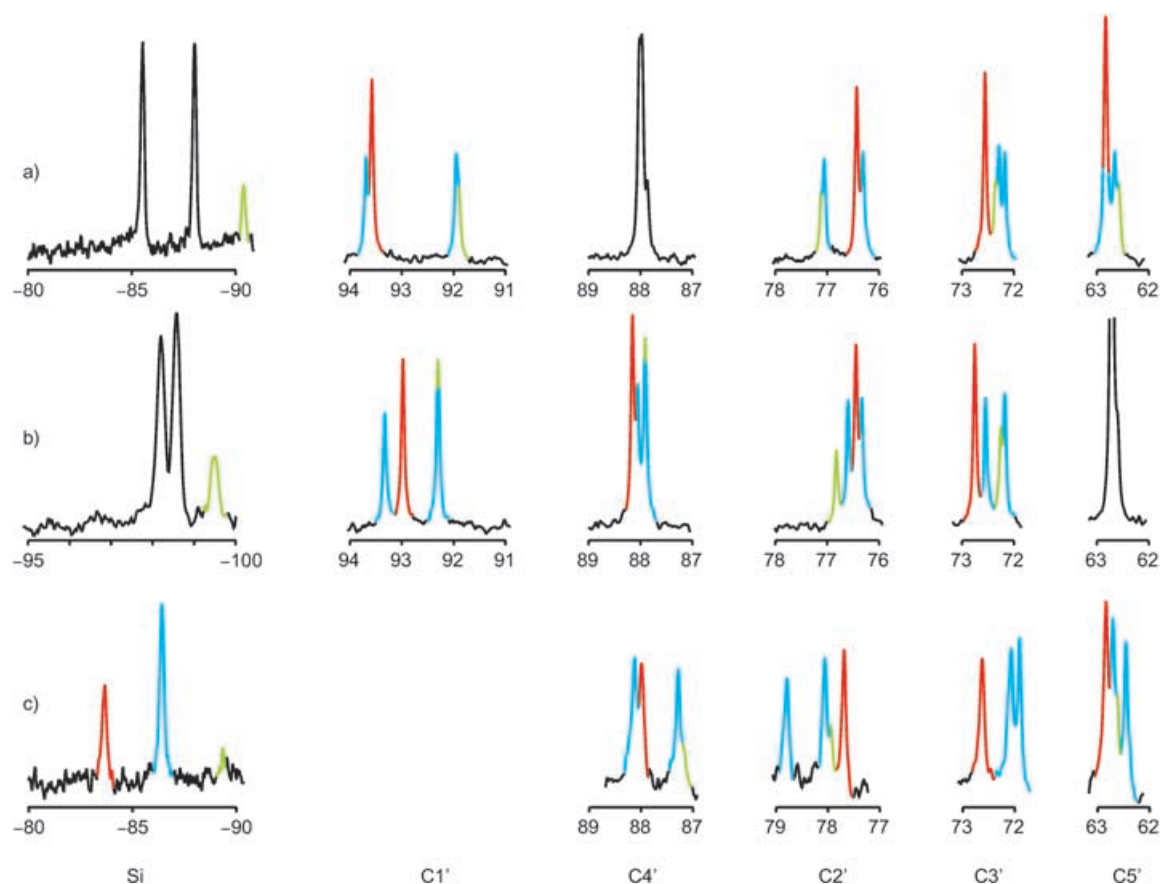


Figure 15. *syn/anti* Isomerism governing the ^{29}Si (left) and ^{13}C NMR spectra of the ribose region in methanolic solutions containing pentacoordinate bis-(nucleosidato)silicates. Molar ratio of nucleoside:[SiR(OMe) $_3$]:methoxide = 2:1:1; counterion: [K([18]crown-6)] $^+$ (Ado) or K $^+$ (Cyd); total Si concentration: 0.20 and 0.36 mol kg $^{-1}$ for Ado and Cyd, respectively. a) [SiPh(Ado2',3'H- $_2$)] $^-$; b) [Si(OMe)(Ado2',3'H- $_2$)] $^-$; c) [SiPh(Cyd2',3'H- $_2$)] $^-$; the C1' signals of Cyd are not shown due to overlap with the C5 signals. Color code: red: *anti/anti*; blue: *syn/anti*; green *syn/syn*.

anol and *N,N*-dimethylformamide yielded ^{13}C NMR spectra which show the isomer of third-highest abundance enriched in terms of the most-upfield phenyl signals. At the same time, *one* of the three main signals of each carbon atom shows increased intensity. Hence, the enriched isomer is assigned as *anti/anti* (Figure 16c). It should be noted that this assignment resembles the AnEryt pattern in the phenyl region. A detailed table of shift differences of individual isomers would be less complete than for Ado. To show the general trend that the largest shift differences are found for the carbons adjacent to the diol group, the mean values of the three strong signals are used. The individual shift differences in this case are 3.4 for C1', 2.3 for C2', 2.1 for C3', 2.8 for C4', and 1.4 ppm for C5'.

Attempts to prepare tetramethoxysilane/methanol solutions as with Ado failed due to the formation of precipitates. On the other hand, aqueous solutions with a 2:1:1 ratio of nucleoside, silica, and hydroxide were possible with Cyd. In comparison with AnEryt, the nucleoside appears to be less suited to forming pentacoordinate silicon than the parent diol in terms of free diol and oxosilicate left. The ^{13}C NMR signals show the usual downfield shift but to a somewhat

lesser extent than with the phenylsilicate. The individual shift differences are 3.0 for C1', 1.7 for C2', 1.6 for C3', 2.6 for C4', and 0.8 ppm for C5'.

As regards ^{13}C NMR shift differences, the N-glycosides Ado and Cyd have watered down the rule emerging from AnEryt but have not completely invalidated it in showing the tendency that the highest values are found for the carbons adjacent to the diol function.

Methyl- β -D-ribofuranoside: Bearing in mind the aim of determining rules for the analysis of ribofuranose–silicate signal patterns, methyl- β -D-ribofuranoside (Me- β -D-Ribf) should add particularly valuable data, since as an O-glycoside it more closely resembles the sugar than a nucleoside does. Reaction of a double molar amount of Me- β -D-Ribf with trimethoxy(phenyl)silane/methoxide in methanol yielded the three expected pentacoordinate silicate species (Figure 16). The ^{13}C NMR signals are not as well resolved as in the case of Ado, but the typical *syn/anti* split can be observed for the diol carbons C2' and C3' (Figure 16). The tendency for the signals of the carbon atoms adjacent to the diol carbons to shift downfield to the largest extent is the

Table 5. Chemical shifts [ppm] in the ^{13}C NMR spectra of solutions of $[\text{K}([18]\text{crown-6})][\text{SiR}(\text{Ado}2',3'\text{H}_{-2})_2]$, and shift differences (δ -(silicate)– δ (free diol)). Bold: $\Delta\delta$ of those carbon atoms that bear the silicon-binding oxygens. For atomic numbering of Ado see Scheme 1. n.d. = not determined due to signal overlap.

		R = Ph		R = OMe	
		δ	$\Delta\delta$	δ	$\Delta\delta$
C1'	<i>anti/anti</i>	93.6	4.0	93.0	3.4
	<i>syn/anti</i> 1	93.7	4.1	93.3	3.7
	<i>syn/anti</i> 2	91.9	2.3	92.3	2.7
	<i>syn/syn</i>	91.9	2.3		
C2'	<i>anti/anti</i>	76.4	2.3	76.4	2.4
	<i>syn/anti</i> 1	77.0	2.9	76.6	2.6
	<i>syn/anti</i> 2	76.3	2.2	76.3	2.3
	<i>syn/syn</i>	77.1	3.0	76.8	2.8
C3'	<i>anti/anti</i>	72.5	1.4	72.8	1.7
	<i>syn/anti</i> 1	72.3	1.2	72.6	1.5
	<i>syn/anti</i> 2	72.2	1.1	72.2	1.1
	<i>syn/syn</i>	72.3	1.2	72.3	1.2
C4'	<i>anti/anti</i>			88.1	1.5
	<i>syn/anti</i> 1	88.0	1.4	88.0	1.4
	<i>syn/anti</i> 2			87.9	1.3
	<i>syn/syn</i>	87.9	1.3		
C5'	<i>anti/anti</i>	62.8	0.9	62.7	0.8
	<i>syn/anti</i> 1				
	<i>syn/anti</i> 2	62.6	0.7		
	<i>syn/syn</i>	62.5	0.6	62.6	0.7
C8	<i>anti/anti</i>	140.8	n.d.	140.7	n.d.
	<i>syn/anti</i> 1	140.8	n.d.	140.7	n.d.
	<i>syn/anti</i> 2	140.1	n.d.	140.4	n.d.
	<i>syn/syn</i>			140.4	n.d.

same as with AnEryt, but the numbers are again different. Using mean values including all three isomers, the shift differences in question are those given in Table 6. Again, the rule is weakened: the C1 signal is no longer the most shifted as the C4 signal shows the largest shift difference.

As an overall result it can be stated that a moderate downfield shift of about 2 ppm of the diol carbons is observable on binding to pentacoordinate silicon. At the same time, a more pronounced downfield shift of one of the adjacent carbons of up to about 5 ppm may occur.

More-pronounced linking of equilibria—ribose in silicate solutions: Up to this point, there has been no doubt about the configuration of the diol in question. A known total concentration of the ligand thus enters the equilibria that describe complex formation and dissociation. This point becomes different when changing from simple diols and glycosides to glycoses. The free ligand is now withdrawn to a large extent from the complex equilibrium by the linked pyranose/furanose and anomeric equilibria of the carbohydrate itself. Compared to AnEryt, the situation is worse for a pure NMR treatment if a glycoside is employed as a silicon ligand in aqueous solution.

Starting with ^{29}Si NMR spectroscopy, it has been demonstrated that the entire transformation of all the oxosilicate

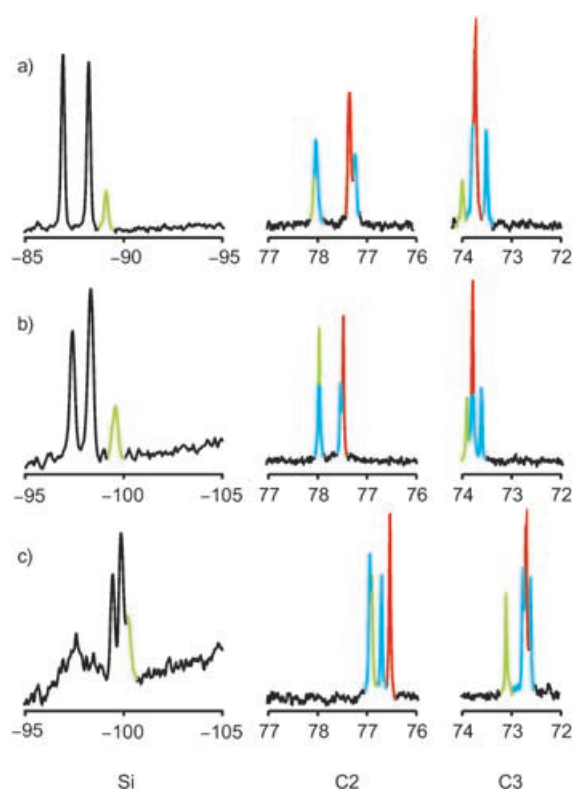


Figure 16. ^{29}Si and ^{13}C NMR spectra (C2 and C3 signals) of 2:1:1 solutions of Me- β -D-Ribf, $\text{SiR}(\text{OMe})_3$, and base. Red: *anti/anti*; blue: *syn/anti*; green: *syn/syn* isomer of the respective $[\text{Si}(\text{R})(\text{Me}-\beta\text{-D-Ribf}2,3\text{H}_{-2})_2]^-$ ion. a) R = Ph; base: KOMe; solvent: methanol. b) R = OMe; base: KOMe; solvent: methanol. c) R = OMe; base: CsOH; solvent: water. Total Si concentration: 0.72, 0.47, and 0.75 mol kg $^{-1}$ for a–c, respectively. The ratio of oxosilicate and pentacoordinate silicate is approximately 3:1.

Table 6. Shift differences (δ (silicate)– δ (free diol)) in the ^{13}C NMR spectra of solutions of $\text{A}[\text{SiR}(\text{Me}-\beta\text{-D-Ribf}2,3\text{H}_{-2})_2]$ prepared with a 2:1:1 molar ratio of the riboside, the silicon starting material, and base. Bold: $\Delta\delta$ of those carbon atoms that bear the silicon-binding oxygens. For atomic numbering of Me- β -D-Ribf see Scheme 1.

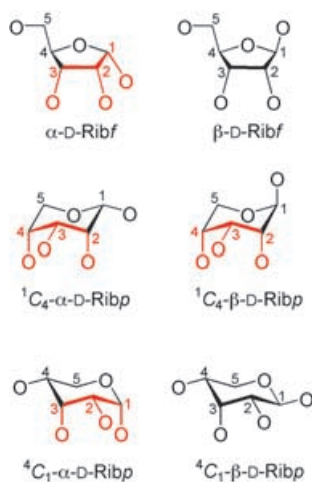
R	solvent	A	C1	C2	C3	C4	C5
Ph	MeOH	K	2.4	2.4	1.9	5.2	0.2
OMe	MeOH	K	1.9	2.0	1.5	4.5	0.0
OH	H $_2$ O	Cs	2.3	2.3	1.8	4.1	0.5

employed into penta- and hexacoordinate diolatosilicates is possible.^[13,14] The experimental conditions for achieving this result include a large excess of aldose and high total concentrations (it should be noted that the 3.3M sugar concentration of reference [14] resembles a syrup, with more than a kilogram of sugar per liter in the case of a disaccharide). In terms of ^{13}C NMR spectra, a proper analysis becomes more difficult due to large amounts of free sugar beside small amounts of Si-bonded glycoside. To demonstrate the specific problems, let us focus on the less basic solutions that have been used by Lambert to detect ribose ligands in pentacoordinate bis(diolato)hydroxosilicate species.^[14] From the viewpoint of glycoside-bonded silicate, these solutions belong to the regime of pentacoordination, and the shifting between

penta- and hexacoordinate species is effected by the molar amount of base. A maximum of pentacoordinate silicate, together with small amounts of oxosilicate, is found close to a molar ratio of 1:1 for silicon and base. The residual oxosilicate vanishes on removing some 20% of base. Hexacoordinate silicates become enriched on drastically increasing the amount of base towards a 1:3 Si:OH⁻ ratio.^[13] The ¹³C NMR spectra of solutions of both kinds are different and both are rather complicated.

Prior to looking for Si-bonded ribose in the respective spectra, the coordination ability of ribose towards silicon centers is assessed in order to have a rough clue of what should be searched for in addition to the established α -Ribf_{1,2} silicon chelator.^[7]

The tentative silicon binding sites of ribose: Scheme 2 summarizes the furanose and pyranose forms that have to be



Scheme 2. O-atom patterns of the various ribose isomers (H atoms omitted); *fac*-tridentate patterns are highlighted in red.

considered. Since there is no experimental evidence yet that open-chain ribose may play a role, this form will not be considered further. Restricting our discussion to diolate binding first, the experimentally substantiated α -Ribf_{1,2} form appears the most suitable in terms of acidity and stereochemistry. For the stereochemical reasons discussed above, pyranose diol functions seem to be less suitable for silicon chelation. α -Ribf_{2,3} and β -Ribf_{2,3} appear suitable in terms of stereochemistry but the most acidic anomeric hydroxy group would be left protonated on 2,3-complexation. It should be noted at this point, however, that increasing the acidity of the ligand is by no means a guarantee of obtaining a chelated silicate of hydrolytic stability. Silicon complexes of the hydroxycarboxylic acids, for example, are hydrolytically sensitive, as has been demonstrated recently by Tacke et al. for hexacoordinate silicates like citratosilicate or oxalatosilicate.^[20] It may thus be important that the ligand of choice bears a sufficient amount of nondelocalized negative charge on its oxygen atoms to compete with the oxo ligands in aqueous silicate solutions.

Inspection of Scheme 2 suggests the consideration of tridentate triolate binding as well, since ribose is particularly rich in isomers that provide O₃ patterns for a facial binding site. More generally, the question arises whether a pyranoidic *cis,cis*-1,2,3-triol moiety may act as a silicon chelator, i.e., whether the unsuitable, but possibly borderline, Si-binding properties of a pyranoidic *cis*-diol are over-compensated by providing a third binding site. Even more generally, is a pyranoidic 1,3-diol a silicon chelator? Since tridentate silicon binding appears to be a particularly unexplored area, it will be assessed very roughly for the current purpose. If pyranoidic triolate binding is of considerable significance, ¹C₄-Me- β -D-Ribp should be able to enrich a silicate solution with six-coordinate species under the usual aqueous alkaline conditions. Experiment shows that Me- β -D-Ribp does not. Thus, pyranoidic triolate binding will not be considered in this discussion. It should, however, be kept in mind that this point needs further clarification, particularly because Me- β -D-Ribp does not include the anomeric hydroxy group in its O₃ pattern and the required ¹C₄ conformation is not predominant in solution. In the same, very preliminary, way, the significance of tridentate α -D-Ribf_{1,2,3} binding is roughly assessed. If these ligands play a dominant role, hexacoordinate [Si(α -D-Ribf_{1,2,3}H₃)₂]²⁻ species will be formed from stoichiometric solutions under nonhydrolytic conditions. However, solutions in methanol of an *n*:1:2 molar ratio of Rib, Si(OMe)₄, and OMe⁻ show hexacoordinate silicate only for *n*=3 but not for *n*=2. We can therefore conclude that the hexacoordinate silicates are mainly tris(diolato) species instead of bis(triolato)silicates, that is, tridentate chelation by ribose does not appear to be a predominant binding mode. (The rationale for using the tetramethoxysilane/methanol system is explained in the next section.)

When restricting the discussion of silicon binding to furanose diol groups, the main contribution should stem from 1,2-deprotonated α -ribofuranose. 1,2-Deprotonated β -ribofuranose, which contains a *trans*-furanoidic diol like anhydro-threitol, is not suited as a chelator. The two remaining silicon-chelating binding sites, α -Ribf_{2,3} and β -Ribf_{2,3}, are derived from diol functions of lower acidity. The β -furanose, however, is more abundant in aqueous equilibria than the α -furanose, which may compensate the lower acidity of its 2,3 site to some extent.

Steps from a well-established phenylsilicate of ribose towards aqueous silicate solutions: The use of AnEryt as a ligand has demonstrated that there is a close resemblance between solutions of the phenylsilicates in methanol and those in water. To derive a sensible signal assignment in the more complicated ribose case, one more step will be taken to arrive at the aqueous medium, as in the case of Me- β -D-Ribf above. Figure 17a shows the spectrum of ribose in methanol, which is close to the aqueous one (Figure 17f). On adding trimethoxyphenylsilane and methoxide according to a final 2:1:1 molar ratio of Rib, SiPh(OMe)₃, and OMe⁻, the α -furanose binds to silicon and becomes the prominent isomer (Figure 17b).^[7] Due to its bonding in the major species, positive

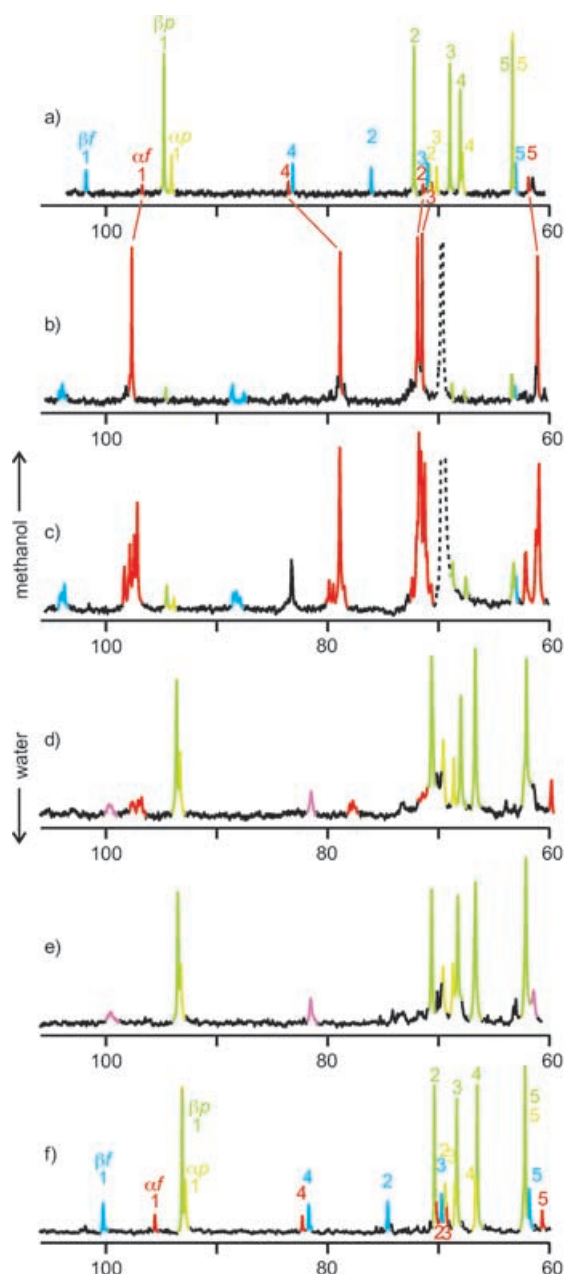


Figure 17. ^{13}C NMR spectra of the ribose region of various aqueous and methanolic solutions. Color codes: red: α -Ribf; blue: β -Ribf; violet: equilibrating α - β -Ribf; green: β -Ribp; yellowish green: α -Ribp. a) Rib in MeOH, $c = 0.2\text{ M}$. b) Reaction mixtures containing a 2:1:1 molar ratio of Rib, $\text{SiPh}(\text{OMe})_3$, and $\text{KOME}/[18]\text{crown-6}$ in MeOH, with the $[\text{PhSi}(\alpha\text{-D-Ribf}1,2\text{H}_{-2})_2]^-$ ion as the main species (red). Total Si concentration: 0.21 mol kg^{-1} . Dashed line: $[18]\text{crown-6}$. c) Reaction mixtures containing a 2:1:1 molar ratio of Rib, $\text{Si}(\text{OMe})_4$, and $\text{KOME}/[18]\text{crown-6}$ in MeOH and containing isomeric forms of the $[\text{Si}(\text{OMe})(\alpha\text{-D-Ribf}1,2\text{H}_{-2})_2]^-$ ion as the main species (red). Total Si concentration: 0.48 mol kg^{-1} . Dashed line: $[18]\text{crown-6}$. d) Aqueous solution of Rib, $\text{Si}(\text{OMe})_4$, and NaOH at a 2:1:1 molar ratio. Total Si concentration: 0.46 mol kg^{-1} ; pH 11.8. e) Rib in NaOH, molar ratio: 1:0.12, total ribose concentration: 0.46 mol kg^{-1} ; pH 11.5. f) Same as (e), but pH adjusted to 6.5 after about 18 h at pH 11.5 at room temperature. Note the weak, unassigned signals around the position of β -Ribf-C2 that indicate some degree of decomposition.

signal assignment is possible with certainty using 2D NMR techniques. In terms of shift differences, the result is disastrous in light of the rules derived up to now. The resonance positions of the ^{13}C NMR signals of α -Ribf in methanol are shifted downfield by 0.9 (C1), 0.5 (C2), 0.9 (C3), -4.6 (C4), and -0.9 ppm (C5) on formation of the $[\text{SiPh}(\alpha\text{-D-Ribf}1,2\text{H}_{-2})_2]^-$ complex ion. The largest shift is that of C4—the carbon with the largest distance from the reaction center within the furanose ring—of more than 4 ppm *upfield*. Although silicon binding through the 1,2-chelate was confirmed by X-ray analysis,^[7] this binding site clearly cannot be recognized from AnEryt-derived shift differences, either from those in reference [14] or from corrected values that are unaffected by the wrong DEPT assignment.

To take a step towards the aqueous silicate solution, methanol is kept as the solvent for the moment but trimethoxyphenylsilane is replaced by tetramethoxysilane. The spectrum with a 2:1:1 ratio of Rib, $\text{Si}(\text{OMe})_4$, and OME^- , is shown in Figure 17c. Again, there is a main species with the same stoichiometry as employed, just as with the phenyl derivative. Signal assignment by two-dimensional techniques is possible as well. Not surprisingly, the order of signals remains the same due to the obvious similarity of the spectra. Keeping to the discussion of the main species, the difference between the phenylsilicate and the tentative methoxosilicate is obvious: each of the five main signals is accompanied, within a 2 ppm range, by weaker signals which adopt a pattern that recalls the spectral features of the *syn/anti* isomers of AnEryt and the β -D-furanosides. It should be noted that the $[\text{SiPh}(\alpha\text{-D-Ribf}1,2\text{H}_{-2})_2]^-$ ion is *anti/anti* in the solid state.^[7] Hence, stability relationships such as those for AnEryt, where *anti/anti* and *syn/anti* isomers are the major species and the *syn/syn* isomer is the minor one, do not appear to be divergent. The spectral properties of the isomer mixture were evaluated as above: one signal for each unique carbon of the ligand for *anti/anti* and *syn/syn*, two signals of about equal intensity for the *syn/anti* isomer, and all the signals of one carbon in a 2 ppm range. Bearing in mind these characteristics, a well-resolved signal such as that for C1 seems to support the idea that *syn/anti* isomerism may occur with ribose as well.

The next step appears to be the most critical. The addition of water to these solutions causes partial hydrolysis and oxosilicate formation. However, the methanol solutions do not appear to be moisture-sensitive in a narrower sense. The addition of a few mols of water per mol of silicon does not alter the spectra significantly, an observation that is in line with Kinrade's and Harris's reports on Si-OH/Si-OME exchange in water/methanol mixtures.^[21] Complete replacement of methanol by water, however, drives oxosilicate formation close to completeness in dilute solutions with a 2:1:1 stoichiometry. At the same time, the equivalent amount of ribose, which occurs as a mixture of its four isomers in the alkaline solution, is set free. Increasing the total concentration allows increasing amounts of pentacoordinate silicate to survive. At the same time, there are no longer equilibrium conditions. For example, 2:1:1 solutions containing

0.46 mol kg⁻¹ Si remain clear for a day but colorless precipitates appear after that time. More-concentrated batches of the 2:1:1 stoichiometry cannot be prepared as clear solutions. A 2:1:1 batch of 0.67 mol kg⁻¹ Si, for example, shows the formation of precipitates during preparation. Lowering the amount of base causes gelation, and increasing the amount of ribose retards gelation. Thus, a solution which resembles the conditions of reference [14] (ca. 3:1:0.8 at a total Si concentration of 1.1 M), gels within half an hour in our laboratory. To come close to this reported Si concentration of 1.1 M, but at the same time to avoid gelation, the spectrum of the 2:1:1 solution with 0.46 mol kg⁻¹ Si was chosen for Figure 17d. Comparison with reference [14] shows the same features for both spectra. To separate the signals of the minor amount of ribose that is still bonded to silicon, the signals of the free sugar have to be recognized as such. Figure 17e shows a ribose spectrum taken at pH 11.5. A comparison with Figure 17d reveals a few signals that are unique to the silicate spectrum, therefore assignment of these signals to the Si-bonded α -Ribf_{1,2} ligand appears sensible. Comparison of Figures 17c and d shows that the C_{2,3,5} signals of Si-chelating α -Ribf are prone to overlap with signals of free ribose. Si-bonded α -Ribf-C₁ and C₄, however, are expected to resonate slightly upfield from their positions in methanol, in regions free of signals of ribose itself. In fact, broad signals are visible at these positions which indicate the presence of the pentacoordinate [Si(OH)(α -Ribf_{1,2}H₂)₂]⁻ species in aqueous solution.

The result of the ribose investigation may be summarized in terms of available methods. Since there is obviously no usable system for shift differences on the basis of the presently available data, the silicon-binding sites of the carbohydrates cannot be determined in solutions that do not allow for unambiguous signal assignment by, preferably, two-dimensional methods. The main problems of an NMR methodology in aqueous glucose chemistry are thus the weak and broad ¹³C NMR signals, owing to small amounts of complexed glucose species, together with the spreading of their signal intensity over several isomers, a problem that is hidden by presenting ²⁹Si NMR spectra that benefit from using glucose in excess.

A strategy to overcome these problems is evident in Figure 17. By the introduction of chemically related systems such as the phenylsilicates/methoxosilicates in methanol, isomerism and hydrolysis, which are the two most critical processes in aqueous solution, may be separated from one another. When using a strategy starting at silicon centers of reduced functionality, it should always be kept in mind that the use of phenylsilicon residues, for example, introduces a (deliberate) bias towards pentacoordinate bis(diolato) species; either pentacoordinate (diolato, triolato) or hexacoordinate bis(triolato) species will be suppressed and have to be considered separately.

Minor species in methanol solutions: In the search for minor products in the ¹³C NMR spectra of Figure 17, two groups of resonances attracted our attention. Both in the phenylsili-

cate and the methoxosilicate solutions a signal group at about $\delta=104$ ppm occurs which can be recognized under aqueous conditions only at higher resolution than that of the figure. A second group occurs at about $\delta=88$ ppm in methanol solution, but is lacking in water. In light of the above considerations, a β -Ribf_{2,3} ligand appears to be a candidate for a second Si-binding site. Data that can support or exclude this suggestion have been presented above. In addition to AnEryt, Me- β -D-Ribf is a suitable ligand for silicon because it enriches a silicate solution with pentacoordinate silicate *under the same experimental conditions* as ribose. Owing to the greater abundance of β -ribofuranose (13.2% in aqueous equilibrium) over the α -isomer (7.4%), it does not appear to be impossible to observe the β -Ribf_{2,3}H₂ ligand as a minor species.^[22] Moreover, the consideration of β -Ribf_{2,3} binding clarifies another reason for signal splitting apart from *syn/anti* isomerism and contributes to an understanding of the actual appearance of the spectra in Figures 17b and c. As β -Ribf_{2,3} is the minor ligand, the predominant solution species which contains this ligand should be *anti/anti*-[SiPh(α -Ribf_{1,2}H₂)(β -Ribf_{2,3}H₂)]⁻ in the phenylsilicate case. Signals of the α -Ribf_{1,2} ligand of this species should thus emerge to the same extent as the β -Ribf_{2,3} signals, and the position of these α -Ribf_{1,2} signals should be close to the signals of the same ligand in the main silicate species. In fact, each signal of the main species rises above a background which has the same appearance as the signals stemming from the β -Ribf_{2,3} ligands. (One point has to be clarified in future work: is the *anti/anti* isomer the only species in the phenylsilicate solutions or is there rapid exchange (the latter appears more probable)?).

A final comment on shift differences in the area of pentacoordinate silicon seems appropriate. On considering β -Ribf_{2,3} binding, the large downfield shift of about 5 ppm of C₄ appears to be most questionable. Although we have demonstrated that shift-difference rules derived from the AnEryt family clearly do not work for Ribf_{1,2} bonding, they appear to be usable for Ribf_{2,3}-derived ligands in the sense that a large shift of the C₄ signal is not ruled out from the beginning. The close structural resemblance of the species to be compared should be noted: AnEryt, the ribosides including the nucleosides, and 2,3-bonding ribofuranose comprise the same atomic pattern, whereas 1,2-bonding ribofuranose does not. With the data available now, shift-difference rules may be used, in a very restricted sense, to verify whether an unexpectedly large shift difference is unprecedented. It should be noted that, in a narrow sense, only equal bonding patterns are compared, a fact that is well-known and frequently used in carbohydrate chemistry.^[23]

Hexacoordinate silicates—preliminary structural results: We have pointed out that the growing body of spectroscopic and structural data regarding pentacoordinate silicon complexes is not paralleled by such data on hexacoordinate silicates. The following section provides some preliminary structural data on furanoside complexes and contributes to the above-mentioned question of 1,3-diolate bonding.

Tris-bidentate 1,2-diolate binding—a crystalline cytidine complex: There are no structural data for either pentacoordinate or hexacoordinate nucleoside–silicon complexes. First X-ray results were therefore obtained in attempts to crystallize a pentacoordinate silicate of a nucleoside. With potassium or cesium as the counterion, thin, weakly diffracting, hexagonal platelets were obtained from solutions of a 2:1:1 molar ratio of cytidine, silica, and cesium or potassium hydroxide. The same crystalline silicate grew from solutions of different stoichiometry, including the 3:1:2 ratio which resembles the formula of a tentative hexacoordinate silicate. Although the crystallization conditions were varied widely, the crystals always proved to be the same and were always of very low quality for X-ray diffraction. Although the structure of the silicate ion in $\text{Cs}_2[\text{Si}(\text{Cyd}2',3'\text{H}_2)_3]\cdot 21.5\text{H}_2\text{O}$ (**10**) was resolved (Figure 18), the structure solution is only preliminary.

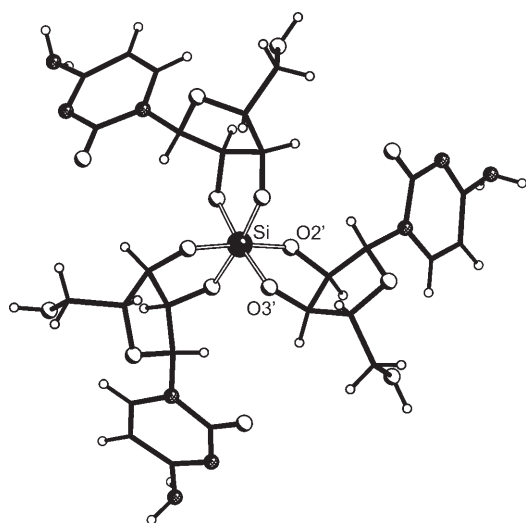


Figure 18. SCHAKAL diagram of the C_3 -symmetrical anions in crystals of **10**. Mean Si–O distance: 1.79 Å. Diol torsion: -27° .

Surprisingly, three $\text{Cyd}2',3'\text{H}_2$ ligands bind to a hexacoordinate silicon center, regardless of the solution composition. The stereochemistry at the silicon atom is Λ . In accordance with the larger apparent radius of the six-coordinate central element, the chelating diol group deviates more strongly from zero torsion. The Si–O distances resemble those in the hexacoordinate silicates of the open-chain sugar alcohols.^[11]

Bis-tridentate 1,3-diolate binding—cis-inositol complexes: The reasons for the furanose-derived diol moieties being the better ligands for small central atoms are restricted to the 1,2-diolate binding mode. Taking into account 1,3-binding, the situation reverses. The bite of a furanoidic 1,3-diolate ligand is relatively large, and thus this coordination mode has been detected in aldose complexation only with a relatively large central atom like palladium(II).^[5] Even simple wire models show that the opposite holds for pyranoidic 1,3-diols, which exhibit a small bite (in a trivial case, a carbon atom matches the central atom site free of strain to com-

plete a second six-membered chair). The finding that a pyranoidic 1,2,3-triol like $^1\text{C}_4\text{-Me-}\beta\text{-D-Ribp}$, with its large torsional angles, is not as efficient an Si-chelator as a furanoidic diol should be contrasted by the significant enrichment of aqueous alkaline silicate solutions by hexacoordinate species on addition of the 1,3,5-triol *cis*-inositol (*cis*-Ins). With cesium as the counterion, crystals of $\text{Cs}_2[\text{Si}(\text{cis-InsH}_3)]\cdot \text{cis-Ins}\cdot 8\text{H}_2\text{O}$ (**11**) were isolated and structurally resolved. Figure 19 shows the bis(triolato)silicate ion.

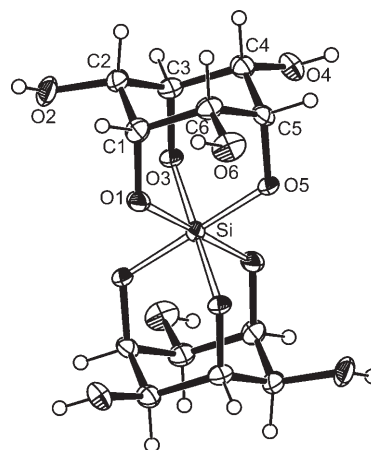


Figure 19. ORTEP diagram (40% probability ellipsoids) of the C_2 -symmetrical anions in crystals of **11**.

Conclusions

Anhydroerythritol: Anhydroerythritol has been introduced primarily as a model compound. In the spirosilane part of this work, however, it was demonstrated for the first time that AnEryt deserves interest in its own right for stabilizing unexpected bonding patterns of silicon. Pentacoordination in a simple silicic acid diol ester appears to be an expression of unsaturated Lewis acidity at the silicon center. Due to the limited “bite” of a diol, the five-membered chelate rings are strained and exhibit O–Si–O angles of about 10° less than the tetrahedral angle. Correspondingly, the expanded tetrahedron edges (O–Si–O ca. 115°) are prone to attack by a Lewis base. In the dimerization reaction that occurs during the crystallization of **6**, the O atoms of the Si–O–C linkages take on the role of the base. This chemistry is thus unique to diols that lack further centers of basicity such as additional hydroxy functions. Pentacoordinate silicic acid dimers are thus not expected to occur as a general bonding pattern in carbohydrate–silicon chemistry as they require special properties of the diol component. We will support this view of a special position for anhydroerythritol and *cis*-cyclopentanediol in due course by means of DFT calculations.^[24]

In the case of the penta- and hexacoordinate silicates, AnEryt is not merely a carbohydrate model of reduced functionality but occupies a special position as well: currently, it is the best suited furanoidic ligand for silicon chelation

in aqueous solution. It should be noted that, compared with AnEryt, reducing sugars such as ribose are silicon chelators of minor affinity,^[13] so preparative use of glucose–silicon chemistry may require nonaqueous solvents. To continue the search for chelate silicates of hydrolytic stability, glycosides with special structural features may be more promising than the parent glycoses themselves. Thus the glycoses' benefit of being about an order of magnitude more acidic than AnEryt or a glycoside appears overcompensated by the problem of the existence of unsuited pyranose and *trans*-furanose isomers in the solution equilibria.

¹³C NMR spectroscopy: Aqueous solutions of glycoses and silicate contain pentacoordinate bis(diolato)hydroxosilicate ions. NMR spectroscopic characterization is complicated mainly because of two effects. First, the signals are split and broadened by isomerism. The *syn/anti* binding of two major ligands is well documented but a second form should be considered as well: the exchange of one of the two major diol ligands for a minor ligand gives rise not only to signals of the minor ligand, which may be well separated from the major ligand's shift but, in addition, slightly shifted signals of the remaining major ligand occur. The result is that the signals of the main complex appear to emerge out of a hump in the background. A strategy to assign the signals of at least the main component has been presented. It is based on chemical variation by, for example, a reduction of the functionality at the silicon center or a change of the solvent. One conceivable method for signal assignment is, however, clearly impossible and leads to wrong assignments:^[14] the Si-binding sites of a carbohydrate cannot be determined by using typical and constant shift differences in ¹³C NMR spectra unless the spectra are taken from closely related compounds whose structures perfectly match the structures in question.

Towards physiological conditions: A major motive for investigating aqueous silicon–carbohydrate chemistry is to contribute to biochemical questions regarding the role of silicon in living organisms. A special topic of current interest deals with silica biomineralization. The relevance of higher-coordinate silicates of polyols and catechols in the biomineralization process has been regarded as unlikely due to the unphysiologically high pH values that are needed for the preparation of such compounds.^[25] This opinion is supported by this work for the case of simple diols and some common glycoses. The penta- and hexacoordinate silicate species dealt with here are clearly species of the alkaline regime. Does it thus make sense to investigate the composition of, and binding sites in, five-coordinate glucose–silicate anions at a pH value as low as possible, say 11.7?^[14] The more general questions are: 1) What is the structure and what are the spectroscopic characteristics of a species? and 2) what is its significance in a physiological environment? Mixing up these two questions may lead to an experimental set-up that contributes convincingly to neither. Consider, say, HPO₄²⁻. To do spectroscopy in aqueous solution, pH 9.5, which is the opti-

mum pH for this species, would be the best choice. In an independent set-up, one could determine the hydrogenphosphate concentration at pH 7 as a significant number for assessing its biochemical relevance. For a newly emerged substance class like the carbohydrate–silicon complexes, it thus appears essential to strictly separate the question of their formulae and structures from the question of their biochemical relevance. It appears more appropriate to us, therefore, to find conditions that show the species in question at a maximum concentration, and not to move towards neutral aqueous solution before having ascertained the structures. A species that is detectable at pH 11.7 may be as meaningless at pH 7 as a species investigated at pH 13. However, collecting unambiguous structural information, even at the “wrong” pH for biochemistry, may unravel bonding principles that are useful in the search for molecules that combine them, thereby opening-up a less heuristic approach to new silicon chelators. In a largely unexplored area such as carbohydrate–(semi)metal chemistry, it is, of course, not straightforward to choose the optimum conditions for a species to be investigated. We have used a simple rationale in this work. If there is information on the stoichiometry of a species, for example from solid-state work, solutions of the same stoichiometry are used to investigate that species. We recommend this procedure not as a dogma, but as the most reasonable starting point for an investigation.

Experimental Section

General: Reagent-grade chemicals were purchased from Fluka and used as supplied. All syntheses were carried out under dry nitrogen using standard Schlenk techniques. Organic solvents were dried and purified according to standard procedures and stored under nitrogen. ¹H, ¹³C{¹H}, and ²⁹Si NMR spectra were recorded at room temperature on a Jeol EX 400 (¹H: 400 MHz; ¹³C: 100 MHz; ²⁹Si: 79.4 MHz) or an Eclipse 500 NMR spectrometer (¹H: 500 MHz; ¹³C: 125 MHz). The spectra were referenced to external SiMe₄. The ¹H and ¹³C signals of pentacoordinate silicate species in methanol were assigned by means of ¹H/¹³C COSY and ¹H/¹³C HMQC experiments. Shift differences are given as δ -(silicate)– δ (free diol). Both kinds of shifts were taken from the same spectrum. In the case of insufficient amounts of starting material in nonaqueous solutions, δ (free diol) was taken from reaction mixtures with a slight excess of diol added.

Anhydroerythritol was prepared according to standard procedures.^[26] X-ray: C₄H₈O₃, *M*_r = 104.105 g mol⁻¹, orthorhombic, *P*₂₁₂₁, *a* = 5.4980(1), *b* = 8.1573(1), *c* = 20.9765(3) Å, *Z* = 8, *R*_w(*F*²) = 0.0760, *S* = 1.095.

L-Anhydrothreitol was prepared according to the literature as well.^[27] X-ray: C₄H₈O₃, *M*_r = 104.105 g mol⁻¹, orthorhombic, *P*₂₁₂₁, *a* = 5.3944(4), *b* = 10.3152(7), *c* = 26.904(3) Å, *Z* = 12, *R*_w(*F*²) = 0.0712, *S* = 0.844.

Ph₂Si(*cis*-ChxdH₂) (1): *cis*-Cyclohexane-1,2-diol (0.09 g, 0.79 mmol) and pyridine (0.17 mL, 2.0 mmol) were dissolved in trichloromethane (13 mL). Dichlorodiphenylsilane (0.17 mL, 0.79 mmol) in trichloromethane (13 mL) was then added dropwise and the suspension was stirred for four days at room temperature. After this time the volume was reduced by three quarters and toluene (20 mL) was added. Precipitated pyridinium chloride was filtered off and the solution volume was reduced to 10 mL in vacuo. Colorless crystals of **1** formed in the course of two days whilst keeping the solution at 4 °C (0.18 g, 0.30 mmol, 77% yield). *M.p.* 191 °C; elemental analysis calcd (%) for C₁₈H₂₀O₂Si: C 72.93, H 6.80; found: C 72.58, H 6.89; ¹³C{¹H} NMR (toluene, 100.5 MHz): δ = 21.7 (C4, C5), 30.4 (C3, C6), 77.5 (C1, C2), 127.7 (phenyl-C3, phenyl-C5),

130.2 (phenyl-C4), 133.6, 132.7 (phenyl-C1), 135.4 ppm (phenyl-C2, phenyl-C6); ^{29}Si NMR (toluene, 79.4 MHz): $\delta = -34.4$ ppm; MS (EI^+ , 70 eV): m/z : 592 [I_2], 516 [I_2 -Ph], 418 [I_2 -Ph-C₆H₁₀O], 337, 296 (**1**), 218 [I -Ph]; X-ray: $M_r = 296.435$ g mol⁻¹, triclinic, $P\bar{1}$, $a = 9.3456(1)$, $b = 9.6991(1)$, $c = 10.6862(2)$ Å, $\alpha = 106.1110(8)^\circ$, $\beta = 95.1714(9)^\circ$, $\gamma = 118.4405(6)^\circ$, $Z = 2$, $R_w(F^2) = 0.1457$, $S = 1.125$.

Ph₂Si((R,R)-trans-ChxdH₂) (2): (R,R)-trans-cyclohexane-1,2-diol (0.11 g, 0.96 mmol) and pyridine (0.20 mL, 2.3 mmol) were dissolved in toluene (13 mL) and heated to 50 °C. Dichlorodiphenylsilane (0.20 mL, 0.96 mmol) in toluene (13 mL) was then added dropwise; pyridinium chloride precipitated immediately. The suspension was stirred for 14 h at 50 °C. The solid was filtered off and the solution volume was reduced to 5 mL in vacuo. Colorless crystals of **2** formed in the course of a few days whilst storing the solution at 4 °C (0.21 g, 0.35 mmol, 74% yield). M.p. 255 °C; elemental analysis calcd (%) for C₁₈H₂₀O₂Si: C 72.93, H 6.80; found: C 72.53, H 6.86; ^{13}C NMR (toluene, 100.5 MHz): $\delta = 24.2$ (C4, C5), 34.1 (C3, C6), 76.9 (C1, C2), 127.6 (phenyl-C3, phenyl-C5), 129.9 (phenyl-C4), 133.9, 132.7 (phenyl-C1), 135.7 ppm (phenyl-C2, phenyl-C6); ^{29}Si NMR (toluene, 79.4 MHz): $\delta = -35.3$ ppm; MS (EI^+ , 70 eV): m/z : 593 [I_2], 516 [I_2 -Ph], 418 [I_2 -Ph-C₆H₁₀O], 337, 319, 296 [**2**], 218 [I -Ph]; X-ray: $M_r = 296.435$ g mol⁻¹, monoclinic, $P2_1$, $a = 10.9794(1)$, $b = 10.1930(1)$, $c = 14.9508(2)$ Å, $\beta = 104.1066(5)^\circ$, $Z = 4$, $R_w(F^2) = 0.1128$, $S = 1.117$.

Ph₂Si(AnErytH₂) (3): Anhydroerythritol (0.30 g, 2.87 mmol) and pyridine (0.54 mL, 6.3 mmol) were dissolved in trichloromethane (20 mL), and dichlorodiphenylsilane (0.60 mL, 2.87 mmol) in trichloromethane (20 mL) was then added dropwise. The suspension was stirred for 16 h at 50 °C. After this time the volume was reduced by three quarters and toluene (20 mL) was added. The pyridinium chloride precipitate was filtered off and the solution volume was reduced to 10 mL in vacuo. Colorless crystals of **3** formed in the course of a few days whilst keeping the solution at 4 °C (0.72 g, 2.54 mmol, 88% yield). M.p. 79 °C; elemental analysis calcd (%) for C₁₆H₁₆O₃Si: C 67.58, H 5.67; found: C 67.72, H 5.74; ^{13}C NMR (toluene, 100.5 MHz): $\delta = 75.2$ (C1, C4), 79.2 (C2, C3), 127.9, 128.0 (phenyl-C3, phenyl-C5), 130.8, 131.1 (phenyl-C4), 131.6, 132.4 (phenyl-C1), 134.8, 135.7 ppm (phenyl-C2, phenyl-C6); ^{29}Si NMR (toluene, 79.4 MHz): $\delta = -1.4$ ppm; MS (EI^+ , 70 eV): m/z : 284 [**3**], 206 [I -Ph], 176 [I -Ph-CH₂O]; X-ray: $M_r = 284.382$ g mol⁻¹, triclinic, $P\bar{1}$, $a = 10.6338(2)$, $b = 10.8232(2)$, $c = 13.2007(3)$ Å, $\alpha = 72.9934(9)^\circ$, $\beta = 85.2784(8)^\circ$, $\gamma = 83.764(1)^\circ$, $Z = 4$, $R_w(F^2) = 0.1717$, $S = 0.998$.

Ph₂Si(L-AnThreH₂) (4): L-Anhydrothreitol (0.09 g, 0.92 mmol) and pyridine (0.17 mL, 2.0 mmol) were dissolved in trichloromethane (15 mL). Dichlorodiphenylsilane (0.10 mL, 0.47 mmol) in trichloromethane (15 mL) was then added dropwise and the suspension was heated for 16 h under reflux. After this time the solution volume was reduced to 7 mL and toluene (20 mL) was added. The pyridinium chloride precipitate was filtered off and the solution volume was reduced to 5 mL in vacuo. Colorless platelets of **4** formed in the course of a few weeks whilst keeping the solution at 4 °C (0.21 g, 0.17 mmol, 56% yield). Elemental analysis calcd (%) for C₁₆H₁₆O₃Si: C 67.58, H 5.67; found: C 67.42, H 5.59; ^{13}C NMR (toluene, 100.5 MHz): $\delta = 73.0$ (C1, C4), 80.0 (C2, C3), 128.0 (phenyl-C3, phenyl-C5), 130.7 (phenyl-C4), 132.0 (phenyl-C1), 136.0 ppm (phenyl-C2, phenyl-C6); ^{29}Si NMR (toluene, 79.4 MHz): $\delta = -29.6$ ppm; MS (EI^+ , 70 eV): m/z : 852 [**4**], 775 [I_2 -Ph], 690, 569 [**4**], 491 [I_2 -Ph], 319, 303, 283 [**4**], 259, 241, 199, 183, 163; X-ray: $M_r = 284.382$ g mol⁻¹, monoclinic, $P2_1$, $a = 10.0849(1)$, $b = 23.5576(4)$, $c = 10.2639(2)$ Å, $\beta = 114.1764(6)^\circ$, $Z = 6$, $R_w(F^2) = 0.1114$, $S = 1.013$.

Ph₂Si(cis-CptdH₂) (5): cis-Cyclopentane-1,2-diol (0.28 g, 2.74 mmol) and pyridine (0.51 mL, 6.03 mmol) were dissolved in toluene (20 mL) and heated to 50 °C. Dichlorodiphenylsilane (0.57 mL, 2.74 mmol) in toluene (20 mL) was then added dropwise; pyridinium chloride precipitated immediately. The suspension was stirred for 14 h at 50 °C. The solid was then filtered off and the solution volume was reduced to 10 mL in vacuo. Colorless platelets of **5** formed in the course of few days whilst keeping the solution at 4 °C (0.71 g, 1.25 mmol, 92% yield). M.p. 132 °C; elemental analysis calcd (%) for C₁₇H₁₈O₂Si: C 72.30, H 6.42; found: C 71.96, H 6.10; ^{13}C NMR (toluene, 100.5 MHz): $\delta = 22.5$ (C4), 35.2 (C3, C5), 80.1 (C1, C2), 128.0 (phenyl-C3, phenyl-C5), 131.0 (phenyl-C4), 131.6,

132.7 (phenyl-C1), 134.9, 135.1 ppm (phenyl-C2, phenyl-C6); ^{29}Si NMR (toluene, 79.4 MHz): $\delta = -3.7$ ppm; ^{29}Si CP/MAS NMR (99.4 MHz): $\delta = -34.7$ ppm; MS (EI^+ , 70 eV): m/z : 564 [**5**], 282 [**5**], 204 [I -Ph], 176 [I -Ph-C₂H₄]; X-ray: $M_r = 282.409$ g mol⁻¹, triclinic, $P\bar{1}$, $a = 9.249(1)$, $b = 9.537(1)$, $c = 10.048(2)$ Å, $\alpha = 83.17(2)^\circ$, $\beta = 68.72(2)^\circ$, $\gamma = 61.08(1)^\circ$, $Z = 2$, $R_w(F^2) = 0.0793$, $S = 0.933$.

α -Si(AnErytH₂) (α -6): Anhydroerythritol (2.97 g, 28.5 mmol) was dissolved in toluene (40 mL) and then tetrachlorosilane (1.63 mL, 14.2 mmol) in toluene (30 mL) was added dropwise within 15 min. A transient colorless precipitate dissolved on completion of the silane addition. After heating for 2 h under reflux, the solution volume was reduced to 10 mL. On keeping the solution at 4 °C, colorless platelets of α -6 formed (2.89 g, 12.4 mmol, 88% yield). M.p. 181 °C; elemental analysis calcd (%) for C₈H₁₂O₆Si: C 41.37, H 5.21, Si 12.09; found: C 41.28, H 5.28, Si 11.90; ^1H NMR (500.2 MHz, [D₈]toluene): $\delta = 2.87$ (m, 4H; H1, H4), 3.79 (m, 4H; H1, H4), 4.06 ppm (m, 4H; H2, H3); ^{13}C NMR ([D₈]toluene, 128.5 MHz): $\delta = 74.9$, 75.0 (C1, C4), 77.6, 77.7 ppm (C2, C3); ^{29}Si NMR ([D₈]toluene, 79.4 MHz): $\delta = -36.7$ ppm; ^{29}Si CP/MAS NMR (99.4 MHz): $\delta = -36.7$ ppm; MS (EI^+ , 70 eV): m/z : 232 [**6**], 231 [I -H], 202 [I -CH₂O], 201 [I -H-CH₂O], 190 [I -C₂H₂O], 189 [I -H-C₂H₂O], 171 [I -H-2CH₂O], 159 [I -H-C₂H₂O-CH₂O]; X-ray: $M_r = 232.263$ g mol⁻¹, orthorhombic, $Pca2_1$, $a = 10.3366(2)$, $b = 10.1473(2)$, $c = 9.1532(1)$ Å, $Z = 4$, $R_w(F^2) = 0.0837$, $S = 1.066$.

β -Si(AnErytH₂) (β -6): Compound α -6 (4.17 g, 18.0 mmol) was sublimed (1 mbar, 120 °C, cold finger: 60 °C). Colorless crystals (3.86 g, 16.6 mmol, 93% yield). M.p.: 181 °C; elemental analysis calcd (%) for C₈H₁₂O₆Si: C 41.37, H 5.21, Si 12.09; found: C 41.12, H 5.47, Si 11.84; ^{29}Si CP/MAS NMR (99.4 MHz): $\delta = -36.6$ ppm; MS (EI^+ , 70 eV): m/z : 232 [**6**], 231 [I -H], 202 [I -CH₂O], 201 [I -H-CH₂O], 190 [I -C₂H₂O], 189 [I -H-C₂H₂O], 172 [I -2CH₂O], 171 [I -H-2CH₂O], 159 [I -H-C₂H₂O-CH₂O]; X-ray: $M_r = 232.263$ g mol⁻¹, orthorhombic, $Pbca$, $a = 8.9325(1)$, $b = 9.1678(1)$, $c = 23.7776(3)$ Å, $Z = 8$, $R_w(F^2) = 0.0828$, $S = 1.058$.

γ -Si(AnErytH₂) (γ -6): Compound α -6 (1.05 g, 4.5 mmol) was dissolved in boiling acetonitrile (2 mL). Colorless crystals formed in the course of few days at 4 °C (0.14 g, 0.6 mmol, 8% yield). *Crystallization succeeded once but has not been reproduced yet!* M.p. 179 °C; elemental analysis calcd (%) for C₈H₁₂O₆Si: C 41.37, H 5.21, Si 12.09; found: C 40.97, H 5.47, Si 11.76; ^{29}Si CP/MAS NMR (99.4 MHz): $\delta = -37.9$ ppm; MS (CI, methane): m/z : 337 [I +AnEryt], 232 [**6**], 189 [I -H-C₂H₂O], 105 [AnEryt+H], 87 [C₄H₂O₂]; X-ray: $M_r = 232.263$ g mol⁻¹, orthorhombic, $Pbca$, $a = 9.3070(1)$, $b = 11.0378(2)$, $c = 19.1601(3)$ Å, $Z = 8$, $R_w(F^2) = 0.1144$, $S = 1.101$.

Si₂(AnErytH₂)₄ (6**)**: Compound α -6 (1.75 g, 7.5 mmol) was dissolved in boiling toluene (5 mL). Colorless crystals of α -6 formed in the course of few days at 4 °C (0.79 g, 1.69 mmol, 45% yield). These crystals were filtered off at 4 °C. Colorless platelets of **6** formed subsequently in the course of a few weeks. M.p. 140 °C; elemental analysis calcd (%) for C₈H₁₂O₆Si: C 41.37, H 5.21, Si 12.09; found: C 41.20, H 5.39, Si 11.97; ^{29}Si CP/MAS NMR (99.4 MHz): $\delta = -94.3$ ppm; MS (CI, methane): m/z : 464 [**6**], 337 [I +AnEryt], 232 [**6**], 105 [AnEryt+H]; X-ray: $M_r = 232.263$ g mol⁻¹, monoclinic, $P2_1/c$, $a = 8.3619(2)$, $b = 16.8394(5)$, $c = 6.9375(2)$ Å, $\beta = 105.5409(12)^\circ$, $Z = 4$, $R_w(F^2) = 0.0852$, $S = 1.052$.

β -Si₂(cis-CptdH₂)₄ (β -7): cis-Cyclopentane-1,2-diol (1.15 g, 11.3 mmol) and toluene (25 mL) were heated to 100 °C. Tetrachlorosilane (0.593 mL, 5.6 mmol) in toluene (25 mL) was then added dropwise within 15 min. A transient colorless precipitate dissolved on completion of the silane addition. After heating for 2 h under reflux, the solution volume was reduced to 5 mL. On keeping the solution at 4 °C, colorless platelets of β -7 formed (1.12 g, 2.5 mmol, 88% yield). M.p. 102 °C; elemental analysis calcd (%) for C₁₀H₁₆O₄Si: C 52.61, H 7.06, Si 12.30; found: C 52.51, H 7.16, Si 12.20; ^1H NMR (500.2 MHz, [D₈]toluene): $\delta = 1.23$ (m, 1H; H5), 1.26 (m, 2H; H1, H4), 1.79 (m, 1H; H5), 4.32 ppm (m, 4H; H2, H3); ^{13}C NMR ([D₈]toluene, 128.5 MHz): $\delta = 20.2$ (C5), 33.5, 33.6 (C1, C4), 76.9, 77.1 ppm (C2, C3); ^{29}Si NMR ([D₈]toluene, 79.4 MHz): $\delta = -36.8$ ppm; ^{29}Si CP/MAS NMR (99.4 MHz): $\delta = -94.6$ ppm; MS (FAB⁺, xenon, NBA, 6 keV): m/z : 457 [**7**], 228 [**7**], 200 [I -C₂H₄], 199 [I -C₂H₃], 171 [I -C₂H₄-C₂H₃]; X-ray: $M_r = 228.317$ g mol⁻¹, monoclinic, $P2_1/c$, $a =$

10.5586(2), $b=10.3715(2)$, $c=9.9903(2)$ Å, $\beta=105.4087(8)^\circ$, $Z=4$, $R_w(F^2)=0.0837$, $S=1.056$.

α -Si(*cis*-CptdH₂)₂ (α -7): Compound β -7 (2.05 g, 4.5 mmol) was sublimed (1 mbar, 60 °C, cold finger: 15 °C). Colorless crystals (1.82 g, 4.0 mmol, 89% yield). M.p. 100 °C; elemental analysis calcd (%) for C₁₀H₁₆O₄Si: C 52.61, H 7.06, Si 12.30; found: C 52.31, H 7.09, Si 12.17; ²⁹Si CP/MAS NMR (99.4 MHz): $\delta=-94.7$ ppm; MS (CI⁺, isobutane): m/z : 457 [7], 228 [7]; X-ray: $M_r=228.317$ g mol⁻¹, monoclinic, $P2_1/c$, $a=10.0605(4)$, $b=11.2398(5)$, $c=9.2031(4)$ Å, $\beta=91.582(2)^\circ$, $Z=4$, $R_w(F^2)=0.1063$, $S=1.099$.

Na[Si(OH)(AnErytH₂)₂] (8a): Silica (0.060 g, 1.0 mmol) and anhydroerythritol (0.312 g, 3.0 mmol) were suspended in a 2 M sodium hydroxide solution (1.0 mL, 2 mmol). Ultrasonication (30 min, 25 °C) yielded a clear solution. Colorless platelets formed on evaporation of the solvent at 4 °C in the course of three months. ²⁹Si NMR (water, 79.4 MHz): $\delta=-97.6$, -98.4 ppm, and oxosilicates; ²⁹Si CP/MAS NMR (99.4 MHz): $\delta=-97.6$ ppm; X-ray: C₈H₁₃NaO₇Si, $M_r=272.260$ g mol⁻¹, triclinic, $P1$, $a=5.741(1)$, $b=6.004(1)$, $c=9.076(2)$ Å, $\alpha=78.03(2)^\circ$, $\beta=89.70(2)^\circ$, $\gamma=61.89(2)^\circ$, $Z=1$, $R_w(F^2)=0.0565$, $S=1.043$.

Rb[Si(OH)(AnErytH₂)₂] (8b): Anhydroerythritol (1.04 g, 10.0 mmol) and tetramethoxysilane (0.61 g, 4.0 mmol) were dissolved in water (10 mL). After the addition of rubidium hydroxide dihydrate (1.05 g, 7.6 mmol) the solution was boiled to evaporate the methanol. Slow evaporation yielded colorless crystals in the course of three weeks. X-ray: C₈H₁₃O₇RbSi, $M_r=334.74$ g mol⁻¹, orthorhombic, $Cmc2_1$, $a=18.701(15)$, $b=6.193(3)$, $c=9.829(4)$ Å, $Z=4$, $R_w(F^2)=0.0955$, $S=1.100$.

Cs[Si(OH)(AnErytH₂)₂] (8c): Anhydroerythritol (0.78 g, 7.5 mmol) and tetramethoxysilane (0.38 g, 2.5 mmol) were dissolved in water (10 mL). After the addition of cesium hydroxide monohydrate (0.88 g, 5.0 mmol) the solution was boiled to evaporate the methanol. Slow evaporation yielded colorless crystals in the course of three weeks. X-ray: C₈H₁₃CsO₇Si, $M_r=382.18$ g mol⁻¹, orthorhombic, $Cmc2_1$, $a=18.629(4)$, $b=6.500(3)$, $c=9.876(2)$ Å, $Z=4$, $R_w(F^2)=0.0874$, $S=1.103$.

K[SiPh(AnErytH₂)₂]-1/2 MeOH (9): A solution of anhydroerythritol (0.231 g, 2.22 mmol), potassium methoxide (0.078 g, 1.11 mmol), and trimethoxyphenylsilane (0.207 mL, 1.11 mmol) in methanol (7 mL) was stirred at 25 °C for 16 h. After concentration of the solution, colorless crystals of **9** formed in the course of a few weeks at 4 °C. ¹³C{¹H NMR (methanol, 67.9 MHz): $\delta=71.5$, 71.9, 72.1 (C2, C3), 74.7, 74.8, 75.3 (C1, C4), 125.6, 126.0, 126.2, 126.5 (phenyl-C3, phenyl-C4, phenyl-C5), 133.7, 134.2, 134.7 (phenyl-C2, phenyl-C6), 143.4, 144.6, 146.2 ppm (phenyl-C1); ²⁹Si NMR (methanol, 79.4 MHz): $\delta=-86.7$, -88.1 , -88.8 ppm. X-ray: C_{14.5}H₁₉KO_{6.5}Si, $M_r=364.486$ g mol⁻¹, monoclinic, $P2_1/n$, $a=15.9982(3)$, $b=10.9630(2)$, $c=18.8191(4)$ Å, $\beta=91.7758(8)^\circ$, $Z=8$, $R_w(F^2)=0.1163$, $S=1.046$.

Cs₂[Si(Cyd2',3'H₂)₃]-21.5 H₂O (10): Silica (0.060 g, 1.0 mmol) and cytidine (0.73 g, 3.0 mmol) were dissolved in 2 M cesium hydroxide (1.0 mL, 2.0 mmol) in an ultrasonic bath. After the addition of acetone (0.2 mL), colorless hexagonal platelets formed within a week at 4 °C. ²⁹Si CP/MAS NMR (79.4 MHz): $\delta=-136.1$ ppm. X-ray: C₂₇H₇₆Cs₂N₉O_{36.5}Si, $M_r=1404.828$ g mol⁻¹, hexagonal, $P6_322$, $a=15.4313(3)$, $c=29.6565(7)$ Å, $Z=4$, $R(F)=0.22$.

Cs₂[Si(*cis*-InsH₃)]-*cis*-Ins-8 H₂O (11): A solution of *cis*-inositol (0.090 g, 0.50 mmol) and tetramethoxysilane (0.037 mL, 0.25 mmol) in 1 M cesium hydroxide (0.50 mL, 0.50 mmol) was stirred at 25 °C for 16 h. After concentration of the solution, colorless crystals of **11** formed in the course of a few weeks at 4 °C. X-ray: C₁₈H₄₆Cs₂O₂₆Si, $M_r=972.439$ g mol⁻¹, triclinic, $P\bar{1}$, $a=10.957(5)$, $b=12.268(5)$, $c=12.501(5)$ Å, $\alpha=83.356(5)^\circ$, $\beta=78.126(5)^\circ$, $\gamma=78.011(5)^\circ$, $Z=2$, $R_w(F^2)=0.0969$, $S=1.058$.

Crystal-structure determination and refinement: Crystals suitable for X-ray crystallography were selected by means of a polarization microscope, mounted on the tip of a glass fiber, and investigated either on a Nonius KappaCCD diffractometer using graphite-monochromated MoK α radiation ($\lambda=0.71073$ Å) or a Stoe IPDS diffractometer using the same radiation. The structures were solved by direct methods (SIR 97, SHELXS) and refined by full-matrix least-squares calculations on F^2 (SHELXL-97). Anisotropic displacement parameters were refined for all non-hydrogen

atoms. CCDC-262917 (AnEryt), CCDC-262918 (L-AnThre), CCDC-262919 (**1**), CCDC-262920 (**2**), CCDC-262921 (**3**), CCDC-262922 (**4**), CCDC-262923 (**5**), CCDC-196570 (α -6), CCDC-196571 (β -6), CCDC-196572 (γ -6), CCDC-196573 (**6**), CCDC-196568 (α -7), CCDC-196569 (β -7), CCDC-262924 (**8a**), CCDC-262926 (**8b**), CCDC-262927 (**8c**), and CCDC-262928 (**10**) contain the supplementary crystallographic data for this paper. These data can be obtained free of charge from the Cambridge Crystallographic Data Center via www.ccdc.cam.ac.uk/data_request/cif.

Computational chemistry: DFT calculations were performed by using the GAUSSIAN 98 and 03 program packages.^[28] The B3LYP/6-31G(d) level of theory was used for geometrical refinement; NMR shifts were calculated at the PBE1PBE/6-311++G(2d,p)//B3LYP/6-31G(d) level.

Acknowledgments

The authors thank Prof. K. Hegetschweiler (Universität des Saarlandes, Saarbrücken) for providing *cis*-inositol, Prof. Dr. J. Senker (Universität Bayreuth) for recording the solid-state NMR spectra, and Prof. Dr. J. Evers (Ludwig-Maximilians-Universität, München) for collecting the X-ray powder data. Part of this work was supported by the focus programme Principles of Biomineralization of the Deutsche Forschungsgemeinschaft.

- [1] G. E. Taylor, J. M. Waters, *Tetrahedron Lett.* **1981**, 22, 1277–1278.
- [2] J. Burger, C. Gack, P. Klüfers, *Angew. Chem.* **1995**, 107, 2950–2951; *Angew. Chem. Int. Ed. Engl.* **1995**, 34, 2647–2649.
- [3] A. Geißelmann, P. Klüfers, B. Pilawa, *Angew. Chem.* **1998**, 110, 1181–1184; *Angew. Chem. Int. Ed.* **1998**, 37, 1119–1121.
- [4] a) R. van den Berg, J. A. Peters, H. van Bekkum, *Carbohydr. Res.* **1994**, 253, 1–12; b) J.-F. Verchere, S. Chapelle, F. Xin, D. C. Crans, *Prog. Inorg. Chem.* **1998**, 47, 837–945.
- [5] P. Klüfers, T. Kunte, *Angew. Chem.* **2001**, 113, 4356–4358; *Angew. Chem. Int. Ed.* **2001**, 40, 4210–4212.
- [6] P. Klüfers, T. Kunte, *Chem. Eur. J.* **2003**, 9, 2013–2018.
- [7] P. Klüfers, F. Kopp, M. Vogt, *Chem. Eur. J.* **2004**, 10, 4538–4545.
- [8] W. Burchard, N. Habermann, P. Klüfers, B. Seger, U. Wilhelm, *Angew. Chem.* **1994**, 106, 936–939; *Angew. Chem. Int. Ed. Engl.* **1994**, 33, 884–887.
- [9] K. Benner, P. Klüfers, J. Schuhmacher, *Angew. Chem.* **1997**, 109, 783–785; *Angew. Chem. Int. Ed. Engl.* **1997**, 36, 743–745.
- [10] a) S. D. Kinrade, J. W. Del Nin, A. S. Schach, T. A. Sloan, K. L. Wilson, C. T. G. Knight, *Science* **1999**, 285, 1542–1545; b) S. D. Kinrade, R. J. Hamilton, A. S. Schach, C. T. G. Knight, *J. Chem. Soc. Dalton Trans.* **2001**, 961–963; c) S. D. Kinrade, A. S. Schach, R. J. Hamilton, C. T. G. Knight, *Chem. Commun.* **2001**, 1564–1565.
- [11] K. Benner, P. Klüfers, M. Vogt, *Angew. Chem.* **2003**, 115, 1088–1093; *Angew. Chem. Int. Ed.* **2003**, 42, 1058–1062.
- [12] K. Benner, P. Klüfers, J. Schuhmacher, *Z. Anorg. Allg. Chem.* **1999**, 625, 541–543.
- [13] S. D. Kinrade, E. W. Deguns, A.-M. E. Gillson, C. T. G. Knight, *Dalton Trans.* **2003**, 3713–3716. Addendum: S. D. Kinrade, R. J. Balec, A. S. Schach, J. Wang, C. T. G. Knight, *Dalton Trans.* **2004**, 3241–3243.
- [14] J. B. Lambert, G. Lu, S. R. Singer, V. M. Kolb, *J. Am. Chem. Soc.* **2004**, 126, 9611–9625.
- [15] O. Seiler, C. Burschka, M. Penka, R. Tacke, *Z. Anorg. Allg. Chem.* **2002**, 628, 2427–2434.
- [16] a) R. E. Ballard, A. H. Haines, E. K. Norris, A. G. Wells, *Angew. Chem.* **1974**, 86, 555–556; *Angew. Chem. Int. Ed. Engl.* **1974**, 13, 541–542; b) R. E. Ballard, A. H. Haines, E. K. Norris, A. G. Wells, *Acta Crystallogr. Sect. B* **1974**, 30, 1590–1593.
- [17] R. G. S. Ritchie, N. Cyr, B. Korsch, H. J. Koch, A. S. Perlin, *Can. J. Chem.* **1975**, 53, 1424–1433.
- [18] D. Schomburg, *Angew. Chem.* **1983**, 95, 52; *Angew. Chem. Int. Ed. Engl.* **1983**, 22, 65.

- [19] R. Tacke, C. Burschka, I. Richter, B. Wagner, R. Willeke, *J. Am. Chem. Soc.* **2000**, *122*, 8480–8485.
- [20] R. Tacke, M. Penka, F. Popp, I. Richter, *Eur. J. Inorg. Chem.* **2002**, 1025–1028.
- [21] a) S. D. Kinrade, K. J. Maa, A. S. Schach, T. A. Sloan, C. T. G. Knight, *J. Chem. Soc. Dalton Trans.* **1999**, 3149–3150; b) A. Samadi-Maybodi, R. K. Harris, S. N. Azizi, A. M. Kenwright, *Magn. Reson. Chem.* **2001**, *39*, 443–446.
- [22] K. N. Drew, J. Zajicek, G. Bondo, B. Bose, A. S. Serianni, *Carbohydr. Res.* **1998**, *307*, 199–209.
- [23] M. J. King-Morris, A. S. Serianni, *J. Am. Chem. Soc.* **1987**, *109*, 3501–3509.
- [24] M. Bootz, P. Klüfers, unpublished results.
- [25] C. C. Perry, D. Belton, K. Shafran, in *Silicon Biomineralization* (Ed.: W. E. G. Müller), Springer, Berlin, **2003**, 269–299.
- [26] F. H. Otey, C. L. Mehlretter, *J. Org. Chem.* **1961**, *26*, 1673.
- [27] J. S. Brimacombe, A. B. Foster, M. Stacey, D. H. Whiffen, *Tetrahedron* **1958**, *4*, 351–360.
- [28] a) Gaussian98 (Revision A.7), M. J. Frisch, G. W. Trucks, H. B. Schlegel, G. E. Scuseria, M. A. Robb, J. R. Cheeseman, V. G. Zakrzewski, J. A. Montgomery, R. E. Stratmann, J. C. Burant, S. Dapprich, J. M. Millam, A. D. Daniels, K. N. Kudin, M. C. Strain, O. Farkas, J. Tomasi, V. Barone, M. Cossi, R. Cammi, B. Mennucci, C. Pomelli, C. Adamo, S. Clifford, J. Ochterski, G. A. Petersson, P. Y. Ayala, Q. Cui, K. Morokuma, D. K. Malick, A. D. Rabuck, K. Raghavachari, J. B. Foresman, J. Cioslowski, J. V. Ortiz, A. G. Baboul, B. B. Stefanov, G. Liu, A. Liashenko, P. Piskorz, I. Komaromi, R. Gomperts, R. L. Martin, D. J. Fox, T. Keith, M. A. Al-Laham, C. Y. Peng, A. Nanayakkara, C. Gonzalez, M. Challacombe, P. M. W. Gill, B. G. Johnson, W. Chen, M. W. Wong, J. L. Andres, M. Head-Gordon, E. S. Replogle, J. A. Pople, Gaussian, Inc., Pittsburgh, PA, **1998**. b) M. J. Frisch, G. W. Trucks, H. B. Schlegel, G. E. Scuseria, M. A. Robb, J. R. Cheeseman, J. A. Montgomery, Jr., T. Vreven, K. N. Kudin, J. C. Burant, J. M. Millam, S. Iyengar, J. Tomasi, V. Barone, B. Mennucci, M. Cossi, G. Scalmani, N. Rega, G. A. Petersson, H. Nakatsuji, M. Hada, M. Ehara, K. Toyota, R. Fukuda, J. Hasegawa, M. Ishida, T. Nakajima, Y. Honda, O. Kitao, H. Nakai, M. Klene, X. Li, J. E. Knox, H. P. Hratchian, J. B. Cross, C. Adamo, J. Jaramillo, R. Gomperts, R. E. Stratmann, O. Yazyev, A. J. Austin, R. Cammi, C. Pomelli, J. Ochterski, P. Y. Ayala, K. Morokuma, G. A. Voth, P. Salvador, J. J. Dannenberg, V. G. Zakrzewski, S. Dapprich, A. D. Daniels, M. C. Strain, O. Farkas, A. D. Rabuck, K. Raghavachari, D. K. Malick, J. B. Foresman, J. V. Ortiz, Q. Cui, A. G. Baboul, S. Clifford, J. Cioslowski, B. B. Stefanov, G. Liu, A. Liashenko, P. Piskorz, I. Komaromi, R. L. Martin, D. J. Fox, T. Keith, M. A. Al-Laham, C. Y. Peng, A. Nanayakkara, M. Challacombe, P. M. W. Gill, B. G. Johnson, W. Chen, M. W. Wong, C. Gonzalez, J. A. Pople, Gaussian03, version B.04, Gaussian, Inc., Pittsburgh PA, **2003**.

Received: February 10, 2005
Published online: August 3, 2005